Saudi Pharmaceutical Journal 29 (2021) 857–873

Contents lists available at ScienceDirect

Saudi Pharmaceutical Journal

journal homepage: www.sciencedirect.com

Original article

Nanoparticles of cisplatin augment drug accumulations and inhibit multidrug resistance transporters in human glioblastoma cells

Naseer Maliyakkal [a,b,c,*], Asmy Appadath Beeran [b], Nayanabhirama Udupa [b]

[a] Department of Basic Medical Sciences, College of Applied Medical Sciences in Khamis Mushait, King Khalid University, Abha, Saudi Arabia
[b] Manipal College of Pharmaceutical Sciences, Manipal Academy of Higher Education, Manipal, Karnataka, India
[c] Cancer Research Unit, King Khalid University, Abha, Saudi Arabia

ARTICLE INFO

Article history:
Received 20 February 2021
Accepted 4 July 2021
Available online 15 July 2021

Keywords:
Cisplatin nanoparticles
Active drug targeting
Targeting multidrug resistance (MDR) transporters
Induction of Apoptosis
Drug uptake and accumulations

ABSTRACT

Background: Cisplatin (CSP) is a potent anticancer drug widely used in treating glioblastoma multiforme (GBM). However, CSP's clinical efficacy in GBM contrasted with low therapeutic ratio, toxicity, and multidrug resistance (MDR). Therefore, we have developed a system for the active targeting of cisplatin in GBM via cisplatin loaded polymeric nanoplatforms (CSP-NPs).

Methods: CSP-NPs were prepared by modified double emulsion and nanoprecipitation techniques. The physiochemical characterizations of CSP-NPs were performed using zeta sizer, scanning electron microscopy (SEM), drug release kinetics, and drug content analysis. Cytotoxicity, induction of apoptosis, and cell cycle-specific activity of CSP-NPs in human GBM cell lines were evaluated by MTT assay, fluorescent microscopy, and flow cytometry. Intracellular drug uptake was gauged by fluorescent imaging and flow cytometry. The potential of CSP-NPs to inhibit MDR transporters were assessed by flow cytometry-based drug efflux assays.

Results: CSP-NPs have smooth surface properties with discrete particle size with required zeta potential, polydispersity index, drug entrapment efficiency, and drug content. CSP-NPs has demonstrated an 'initial burst effect' followed by sustained drug release properties. CSP-NPs imparted dose and time-dependent cytotoxicity and triggered apoptosis in human GBM cells. Interestingly, CSP-NPs significantly increased uptake, internalization, and accumulations of anticancer drugs. Moreover, CSP-NPs significantly reversed the MDR transporters (ABCB1 and ABCG2) in human GBM cells.

Conclusion: The nanoparticulate system of cisplatin seems to has a promising potential for active targeting of cisplatin as an effective and specific therapeutic for human GBM, thus eliminating current chemotherapy's limitations.

Abbreviations: ABC, ATP-binding cassette; ANOVA, Analysis of variance; BBB, Blood brain barrier; BCRP, Breast cancer resistance protein; CSP, Cisplatin; CSP-NPs, Cisplatin nanoparticles DMEM, Dulbecco's modified eagle medium; DMSO, Dimethyl sulfoxide; DNR, Daunorubicin; DOX, Doxorubicin; EDTA, Ethylenediaminetetraacetic acid; EPR, Enhanced permeability retention; FACS, Fluorescence activated cell sorting; FBS, Fetal bovine serum; FTC, Fumitremorgin C; GBM, Glioblastoma multiforme; HBSS, Hank's balanced salt solution; HPLC, High Performance Liquid Chromatography; MDR, Multidrug resistance; MTT, Methyl tetrazolium; MX, Mitoxantrone; nm, Nanometer; NPs, Nanoparticles; O.D., Optical density; PBS, Phosphate buffer saline; PI, Propidium iodide; PLGA, Poly (lactic-co-glycolic) acid; Rho-123, Rhodamine 123; RT, Room temperature; SDS, Sodium dodecyl sulfate; SEM, Scanning electron microscopy.

* Corresponding author at: Dr. Naseer Maliyakkal, Assistant Professor, Department of Basic Medical Sciences, College of Applied Medical Sciences in Khamis Mushait, King Khalid University, Abha, Saudi Arabia.

E-mail addresses: nkassim@kku.edu.sa (N. Maliyakkal), asmyab@gmail.com (A. Appadath Beeran), n.udupa@manipal.edu (N. Udupa).

Peer review under responsibility of King Saud University.

Production and hosting by Elsevier

https://doi.org/10.1016/j.jsps.2021.07.001

1. Introduction

Glioblastoma multiforme (GBM) is a hostile type of cancer and is a malignancy of the glial cells of the brain (Anthony et al., 2019). GBM is characterized by prevalent invasion throughout the brain parenchyma, robust angiogenesis, significant heterogeneity, highly metastatic, and survival is typically three months without treatment (Malinovskaya et al., 2017). Surgery, radiotherapy, chemotherapy remain the mainstay of the GBM treatments. However, GBM is highly resistant to conventional therapies, and the average survival time of GBM patients is only 12–15 months (Liao et al., 2019). Cisplatin (CSP) is a conventionally used anticancer drug with potent cytotoxic effects and an established radio-sensitizer against solid tumors, including GBM (Ghosh, 2019). However, the clinical utility of CSP is limited by the reduced ability of the drug to cross the blood–brain barrier (BBB), intrinsic/acquired drug resistance, development of multidrug resistance (MDR) mechanisms by cancer cells, dose-limiting normal tissue toxicity (neurotoxicity, nephrotoxicity, ototoxicity, hepatotoxicity, and gastrointestinal disturbances), and low bioavailability (only < 10% of the drug fraction free to exert antitumor effects due to irreversible binding to plasma proteins) (Ghosh, 2019; Heffron, 2016; Robey et al., 2018).

Among the various strategies identified to overcome these, the use of polymeric nano-sized carriers has shown a high tumor-targeting ability with enhanced drug delivery without redesigning a drug's molecular structure (Moreno et al., 2010). Polymer-drug conjugates were extensively studied as nanoparticulate based drug delivery systems and found to be effective in anticancer drug targeting as they are biodegradable, compatible, do not accumulate in the body, and are non-toxic (Farooq et al., 2019). Moreover, the physicochemical properties of polymeric nanoparticles (NPs) such as different size (<200 nm), sizeable surface-volume ratio, enhanced permeability retention (EPR) in cancer cells, tumor extravasation, self-assembly, specificity, drug encapsulation, and biocompatibility make them most suitable for anticancer drug targeting (passive targeting) (Masood, 2016). Interestingly, polymeric nanocarriers prolong the in vivo circulation time, reduce cellular uptake to the endocytic route, and enhance the delivery of drugs to tissues with leaky blood vessels (particularly in tumors), and thus improves the undesirable dose-limiting normal tissue toxicity associated with conventional chemotherapy (active targeting) (Hartshorn et al., 2018).

Poly (lactic-co-glycolic acid) (PLGA) is the most effective as a polymeric carrier and modifier for targeted and increased delivery of anticancer drugs as they are biocompatible, biodegradable, allow a sustained drug release, enhance drug effects, reduce adverse effects, and are already approved by the Food and Drug Administration (FDA) and the European Medicines Agency (EMA) (Duan et al., 2016; Moreno et al., 2008). Recent literature suggests that CSP loaded PLGA NPs have the potential to lessen the adverse effects without affecting drug efficacy in a tumor model in mice (Tian et al., 2017). CSP-loaded poly(lactic-co-glycolic) nanoplatforms have shown enhanced internalization and cytotoxicity as compared to free CSP in HER2 targeted ovarian cancer cells (Domínguez-Ríos et al., 2019). NPs prepared from PLGA-β-poly (ethylene glycol) (PLGA-PEG) have shown increased drug accumulations with improved anticancer properties (Mattheolabakis et al., 2009; Gryparis et al., 2007). Aptamer functionalized Pt (IV) prodrug-PLGA-PEG nanoparticles formulation enabled the release of active CSP inside the prostate cancer cells with enhanced cytotoxic effects (Dhar et al., 2008). The cholesterol-CSP-incorporated PLGA-PEG NPs exhibited sustained drug release, increased uptake, tumor growth inhibition, and negligible toxicity (Cheng et al., 2015). Similarly, platinum prodrug-PLGA-PEG NPs caused enhanced drug accumulations in tumor-associated macrophages with controlled drug release effects in tumor cells (Miller et al., 2015). The codelivery of CSP prodrug with siRNAs using PLGA-PEG produced a synergistic effect (Xu et al., 2013). The systemic toxicity of CSP-poly (L-glutamic acid)-g-methoxy PLGA NPs were found to be less in contrast to free CSP in the lewis lung carcinoma (LLC) model (Yu et al., 2016). PLGA nanoparticles system as a 'dual RNAi delivery system,' which contains both MDR1 and BCL2 siRNA, has revealed simultaneous inhibition of drug efflux and cell death defense pathways, thereby overcoming chemoresistance in ovarian cancer cells (Risnayanti et al., 2018). CSP-methoxy-PEG-PLGA NPs have been shown to alter drug distribution with less toxic effects in the kidney (Wang et al., 2013). Similarly, CSP PLGA NPs, prepared by the electrohydrodynamic atomization (EHDA) method, have imparted sustained release effects and induced apoptosis in cancer cells (Reardon et al., 2017). The hyaluronic acid (HA) modified CSP PLGA NPs enhanced anticancer effects by targeting CD44 receptors, which were overexpressed in cancer cells (Alam et al., 2017). CSP-loaded folic acid-PLGA NPs exhibited a sustained release effect with improved anticancer activities in lung and ovarian cancer cells (Tian et al., 2017; Cheng et al., 2011).

Though several reports suggest the efficacy of CSP PLGA NPs to target multiple cancer types, there is no study to elucidate their anticancer mechanism in human GBM cells. Therefore, in this study, we have developed CSP loaded PLGA NPs (CSP-NPs) by double emulsion and nanoprecipitation techniques. The optimized CSP-NPs were characterized for the physicochemical properties (size, zeta potential, polydispersity index, drug encapsulation efficiency, and drug content), morphological features, and the drug release kinetics. CSP-NPs were assessed for their cytotoxic effects in human GBM cells (U-343 and LN-229) and healthy brain neuronal cells (HCN-2). Further, the mechanisms of cell death in cancer cells were studied by apoptosis assay and cell cycle analysis. The potential of CSP-NPs to be taken up explicitly by GBM cells resulting in an increased intracellular accumulation (active targeting) was gauged by fluorescent imaging and flow cytometry-based drug accumulation assays. The recent reports have demonstrated that NPs have the potential to reverse MDR transporters (ABCB1 or p-glycoprotein) by promoting receptor-mediated endocytosis (Bar-Zeev et al., 2017). Moreover, the reversal of MDR in cancer cells by inhibiting the drug efflux transporters (ABCB1 or p-glycoprotein, ABCG2, or BCRP) is an attractive approach to deliver anticancer drugs in cancer cells by active targeting (Appadath Beeran et al., 2014, 2015; Maliyakkal et al., 2015). Therefore, the current study also investigated the potential of CSP-NPs to reverse the MDR transporters in human GBM cell lines.

2. Materials and methods

2.1. Materials

Poly (D, L-lactic-co-glycolic acid) (PLGA) polymer 50:50 (Resomer 503H) (Boehringer Ingelheim, Germany). Cisplatin, polyvinyl alcohol, sodium cholate, methyl tetrazolium, doxorubicin, daunorubicin, Hoechst 33342, dimethyl sulfoxide, propidium iodide, RNase A, rhodamine 123, verapamil, mitoxantrone, fumitremorgin C, dialysis membrane sac, Dulbecco's modified eagle medium, Trypsin-EDTA, Hank's balanced salt solution, human epidermal growth factor, hydrocortisone, insulin, and heparin (Sigma-Aldrich, St. Louis, MO, USA). Fetal bovine serum and B27 (Gibco-Invitrogen, Carlsbad, CA, USA). The cell culture flasks and multi-well plates were obtained from Greiner Bio-One,

Frickenhausen, Germany. HPLC grade solvents were purchased from Merck, Burlington, USA.

2.2. The analytical method for the estimation of cisplatin using High-Performance Liquid Chromatography (HPLC)

A sensitive HPLC method was developed and validated for the quantification of CSP with modifications (El-khateeb et al., 1999). HPLC system (Shimadzu, Kyoto, Japan) with a dual-wavelength UV spectrophotometer detector was used for the estimation of CSP-NPs. The mobile phase consists of an aqueous mobile phase with 3% v/v methanol, 0.05 mM SDS, and pH 2.5 (adjusted with triflic acid) using Grace vydac C18 column (250 × 4.6 mm, 5μ) as stationary phase, maintained at 37 °C with, the flow rate of 0.50 ml/min, and injection volume of 100 μL at a detection wavelength of 305 nm.

2.3. Formulation and development of cisplatin nanoparticles

2.3.1. Nanoparticles prepared by 'Double emulsion solvent evaporation' technique (CPGE)

CSP-loaded PLGA nanoparticles (CPGE) were prepared by water-oil-water (w/o/w) emulsion solvent evaporation method, as reported earlier with modification (Domínguez-Ríos et al., 2019). Briefly, CSP (10 mg) in 2.0 ml of normal saline was emulsified with PLGA 50:50 (100 mg) in dichloromethane by homogenization and probe sonication (amplitude of 80, a pulse of 4 sec) for 10 min with constant stirring at a speed of 1000 rpm. The primary w/o emulsion was then transferred dropwise to an aqueous solution (20 ml) with (1% w/v sodium cholate) with homogenization (Polytron Mixer, Kinematica) at a speed of 15,000 rpm followed by sonication in an ice water bath using probe sonicator at an amplitude of 80, a pulse of 4 sec at a stirring speed 1000 rpm for 10 min to get a w/o/w emulsion. The stable emulsion was stirred for 12 h for the removal of organic solvent. CSP nanoparticles (CPGE) were separated by centrifugation at 20,000 rpm for 5 min, washed with saline, lyophilized (using 5% w/v mannitol as lyoprotectant to prevent the aggregation of the nanoparticles and retain their re-dispersibility), and stored at 4 °C prior to the following use **(Fig. S3)**.

2.3.2. Nanoparticles prepared by 'Nanoprecipitation technique' (CPGN)

CSP-loaded PLGA nanoparticles (CPGN) were also prepared by the nanoprecipitation/solvent diffusion method, as described earlier with modification (Miladi et al., 2016). Briefly, CSP (10 mg) and PLGA 50:50 (100 mg) were dissolved in DMSO (1 ml). The obtained organic solution was added dropwise into (with a microneedle) an aqueous solution (10 ml) containing sodium cholate (1% w/v) under gentle stirring at room temperature to enable the formation of nanoparticles at the solvent interface due to interfacial phenomena. The DMSO in solution was entirely removed by dialysis. This solution was passed through a membrane filter (0.22 μ) to eliminate the non-incorporated drug and polymer aggregates. Solutions of CSP-loaded nanoparticles were then lyophilized (mannitol 5% w/v) for further characterization and utilization. CSP nanoparticles (CPGN) were stored at 4 °C prior to the following use **(Fig. S4)**.

2.4. Characterization of cisplatin nanoparticles

2.4.1. Size and zeta potential analysis

CSP nanoparticles (CPGE and CPGN) were resuspended in 1.0 ml of phosphate buffer saline (PBS) and characterized for particle size (PS), zeta potential (ZP), polydispersity index (PDI) using Zetasizer (Nano ZS, Malvern Instruments, UK).

2.4.2. Scanning electron microscopy (SEM)

The surface morphology of CSP nanoparticles (CPGE and CPGN) were studied using SEM. Briefly, CPGE and CPGN were applied to a metallic cylinder and dried. Subsequently, the samples were coated with gold using an ion sputter (5 mA for 15 min). Samples were assigned to an electron microscope using a sample holder. The surface morphology of nanoparticles was monitored at a voltage of 15 kV (JSM-T20, Kyoto, Japan).

2.4.3. Determination of drug loading and entrapment

The efficiency of drug entrapment and loading were assayed by the HPLC method. Briefly, lyophilized samples (CPGE and CPGN) were suspended in dichloromethane: methanol (8:2) and vortexed for 10 min. The organic solution was entirely evaporated with a nitrogen purge. The residue was reconstituted in millipore water, filtered through the 0.22 μ filter, and 100 μL of the solution was injected into HPLC for the estimation CSP. The percentage drug entrapment efficiency was calculated by the amount of drug present in nanoparticles divided by the initial amount of drug taken multiplied by 100%. Similarly, the percentage of drug loading was estimated by the amount of drug present in nanoparticles divided by the nanoparticles yield multiplied by 100.

2.5. In vitro drug release

Drug release kinetics of CSP nanoparticles in comparison with free CSP were determined using the dialysis sac method (Yu et al., 2019). Briefly, lyophilized CPGE and CPGN were suspended in PBS (0.10 M at pH 7.4). The solution was then placed into a pre-swelled dialysis bag with a 12-kDa molecular weight cutoff and immersed into 20 ml of PBS (pH 7.4) at 37 °C with gentle agitation. At a predetermined time (0–192 h), an aliquot of the nanoparticle suspension (1 ml) was withdrawn by replacing the equal volume of fresh PBS. These samples were separated by centrifugation (5000 rpm for 2 min) and filtered through a membrane filter (0.45 μ). HPLC determined the drug concentration in each sample. The data were represented as the percentage of cumulative CSP release versus time.

2.6. Cell culture

Human glioblastoma (U-343 and LN-229) and brain neuronal (HCN-2) cell lines were cultured in DMEM (high glucose with four mM L-glutamine) with FBS (10%), penicillin (1 kU/ml), and streptomycin (100 μg/ml). The cell lines were procured from American Type Culture System (ATCC) and were found to be without mycoplasma contamination.

2.7. Cytotoxicity assay in human glioblastoma cell lines

Cytotoxic effects of CSP nanoparticles (CPGE and CPGN) in human glioblastoma cells (U-343 and LN-229) and healthy human brain neuronal cell lines (HCN-2) were measured by MTT assay (Averineni et al., 2012). Briefly, U-343, LN-229, and HCN-2 cells cultured at 40–50% confluency were treated with CSP nanoparticles (CPGE and CPGN) (0.1, 1, 10, 50, and 100 μg/mL), free CSP (positive control) and blank NPs (vehicle control) in triplicates for both 48 and 96 h, respectively. Subsequently, MTT solution (5 mg/mL) was added to each well and incubated for 4 h. The formazan was solubilized in DMSO, and the O. D values were measured at 570/630 nm. Cell viability (%) was determined by dividing optical density (O.D.) of the test by O.D. of vehicle control (blank NPs) multiplied by 100. IC_{50} (concentration of the drug required to reduce the percentage of cell viability to 50) values of CSP, CPGE, and CPGN were obtained from the % cell viability versus concentration

plot by non-linear regression analysis using GraphPad Prism Software.

2.8. Detection of apoptosis

The trigger of apoptosis with CSP nanoparticles (CPGE and CPGN) treatment was detected by Hoechst 33342 assay (Appadath Beeran et al., 2015). Briefly, human glioblastoma cells (U-343 and LN-229) cultured at 50–60% confluency were treated with CSP nanoparticles (CPGE and CPGN), free CSP, and blanks NPs (vehicle control) for 96 h. Following the treatment, cells were collected and washed with HBSS twice (by centrifugation at 2,000 rpm for 5 min at RT). Cells were then stained with Hoechst 33342 (2 μg/mL) for 10 min at 37 °C. Subsequently, cells were washed with ice-cold HBSS, and apoptosis was measured using a fluorescent microscope.

2.9. Cell cycle analysis

Cell cycle analysis was performed based on propidium iodide (PI) staining, followed by DNA analysis using flow cytometry (Maliyakkal et al., 2013). Briefly, human glioblastoma cells (U-343 and LN-229) cultured at 40–50% confluency were treated with CSP nanoparticles (CPGE and CPGN), free CSP, and blank NPs (vehicle control) for 96 h. Subsequently, a single-cell suspension was washed with HBSS twice and added 70% ice-cold ethanol dropwise and stored at minus 20 °C. While processing the sample for PI staining, the ethanol was removed entirely by washing with HBSS twice. Cells were treated with RNase A (100 μg/mL) at 56 °C for 3 h, followed by staining with PI at RT for 15 min. The samples were analyzed using flow cytometry (FACSCanto II, BD, USA).

2.10. Drug uptake assay using fluorescent microscopy

Drug uptake of CSP nanoparticles in cancer cells were monitored using cellular uptake assay. Briefly, human glioblastoma cells (U-343 and LN-229) cultured at 40–50% confluency treated with CSP nanoparticles (CPGE and CPGN), free CSP, and blank NPs (vehicle control) for 96 h, with or without the sub-lethal concentration of DOX (0.2 μM). At the end of the treatment, cellular uptake and trafficking of doxorubicin were monitored using a fluorescent microscope (Leica, Germany).

2.11. Drug accumulation assay using flow cytometry

A flow cytometry-based drug uptake assay was used for the measurement of CSP nanoparticles content in the cells (Beeran et al., 2014). Briefly, human glioblastoma cells (U-343 and LN-229) were treated with CSP nanoparticles (CPGE and CPGN), free CSP, and blank NPs (vehicle control) with DNR (2 μM) for 90 min (in DMEM with 2 %FBS). Consequently, cells were resuspended in HBSS at 4 °C. The samples were analyzed by a flow cytometer (FACSCanto II, BD, USA).

2.12. Rhodamine 123 (Rho-123) assays

ABCB1 (p-glycoprotein) inhibitory activity of CSP nanoparticles was evaluated by Rho-123 assay (Maliyakkal et al., 2015). Briefly, human glioblastoma cells (U-343 and LN-229) were stained with Rho-123 (0.50 μM) at standard cell culture conditions (in DMEM with 2% FBS) for 30 min (accumulation phase). Subsequently, after washing with HBSS, cells in the culture medium were treated with CSP nanoparticles (CPGE and CPGN), free CSP, verapamil (50 μM), and blank NPs (vehicle control) without Rho-123 for 60 min (efflux phase) at 37 °C. Thereafter, cells were suspended in HBSS at 4 °C after washing out the Rho-123. The samples were analyzed by a flow cytometer (FACSCanto II, BD, USA).

2.13. Mitoxantrone (MX) assay

ABCG2 reversal activity of CSP nanoparticles was assessed by mitoxantrone (MX) assay (Appadath Beeran et al., 2014; Appadath Beeran et al., 2015). Briefly, human glioblastoma cells (U-343 and LN-229) were stained with MX (10 μM) at standard cell culture conditions (in DMEM with 2% FBS) for 30 min (accumulation phase). Subsequently, after washing with HBSS, cells in culture medium were treated with CSP nanoparticles (CPGE and CPGN), free CSP, fumitremorgin C (10 μM), and blank NPs (vehicle control) without MX for 60 min (efflux phase) at 37 °C. Thereafter, cells were suspended in HBSS at 4 °C after washing out the MX. The samples were analyzed by a flow cytometer (FACSCanto II, BD, USA).

2.14. Statistical analysis

The values are denoted as the SEM of three independent experiments. Statistical evaluation performed using GraphPad Prism 5.0 (GraphPad Software). ANOVA followed by 'Dunnett's multiple comparisons test' and 'Bonferroni post-tests,' were employed to assess the level of statistical significance ($p < 0.05$).

3. Results

3.1. Estimation of cisplatin concentration in the nanoparticulate system

CSP concentrations in the nanoparticulate system were quantified using HPLC. Various experimental parameters (Stationary phase, the composition of the mobile phase, detection wavelength, flow rate, and injection volume) were evaluated. An optimized method developed using a C_{18} column (250 × 4.6 mm, 5μ), which maintained at 37 °C. The mobile phase consists of an aqueous solution of SDS (0.05 mM) with methanol (3% v/v) at pH 2.5 (adjusted with triflic acid). At a detection wavelength of 305 nm, a flow rate of 0.5 ml/min, and an injection volume of 100 μL, the CSP peak was well-resolved with a retention time (Rt) of 5.60 min (**Fig S1**). A plot of peak area versus concentration demonstrated a linear curve with a limit of detection at 0.50 μg/mL (r^2 = 0.999) (**Fig. S1**). Hence, this method was used for the precise estimation of CSP in nanoparticulate systems.

3.2. Cisplatin nanoparticles have desired particle size, zeta potential, and drug content

Formulation and development of CSP nanoparticles were carried out using the modified double emulsion evaporation (w/o/w) method and nanoprecipitation techniques. Various formulation parameters were optimized to get the desired physiochemical properties for the nanoparticles. Among the various batches of CSP nanoparticles prepared, CPGE (prepared by double emulsion (w/o/w) solvent evaporation technique) and CPGN (prepared by nanoprecipitation technique) were selected for further physiochemical characterizations.

3.2.1. Particle size and zeta potential

The optimized CSP nanoparticles (CPGE and CPGN) were assessed for their particle size (PS), zeta potential (ZP), and polydispersity index (PDI) using Zetasizer. The particle size of CPGE and CPGN were 150 ± 10.57 nm and 175.10 ± 5.92 nm, respectively (**Fig. 1 A and B;** Table 1). Similarly, the zeta potential of CPGE

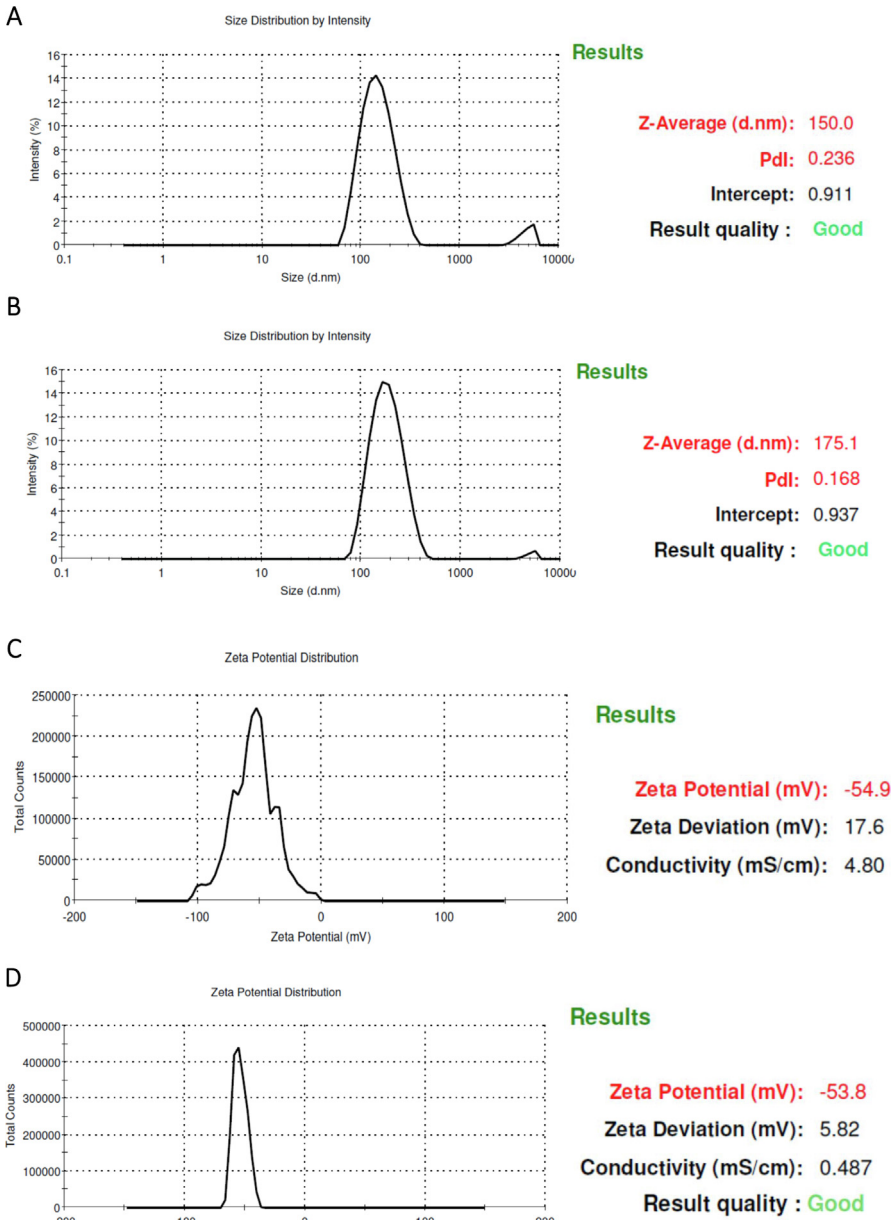

Fig. 1. Cisplatin nanoparticles have desired particle size, zeta potential, and drug content. The nanoparticles of cisplatin (CPGE and CPGN) were analyzed for their particle size (PS), zeta potential (ZP), and polydispersity index (PDI) using Malvern zeta sizer. **A**. Particle size intensity of CPGE. **B**. Particle size intensity of CPGN. **C**. Zeta potential distribution of CPGE. **D**. Zeta potential distribution of CPGN. The images are representative of three independent experiments.

Table 1
Physiochemical properties of cisplatin nanoparticles. The optimized nanoparticle formulations of cisplatin (CPGE and CPGN) were analyzed for the particle size (PS), zeta potential (ZP), and polydispersity index (PDI) using Malvern zeta sizer (Figure 1). Drug entrapment and loading efficiency of CPGE and CPGN were determined by HPLC. Numerical data represent the mean ± standard error of the mean of three independent experiments.

	Particle size (nm)	Zeta potential (mV)	Polydispersity index	Drug entrapment efficiency (%)	Drug loading content (%)
Cisplatin Nanoparticles (CPGE)	150 ± 10.57	−54.90 ± 2.50	0.236 ± 0.05	48.63 ± 4.14	5.67 ± 0.52
Cisplatin Nanoparticles (CPGN)	175.10 ± 5.92	−53.80 ± 4.60	0.168 ± 0.03	45.13 ± 3.25	5.38 ± 0.33

and CPGN were −54.90 ± 2.50 mV and −53.80 ± 4.60 mV, respectively (Fig. 1 **C and D;** Table 1). The polydispersity index for CPGE and CPGN were found to be 0.236 ± 0.05 and 0.168 ± 0.03, respectively (Table 1). Therefore, these data revealed that the optimized nanoparticulate formulations of CSP harbor the desired particle size (<200 nm), polydispersity index (<0.10), and zeta potential (>-60 mV).

3.2.2. Drug entrapment efficiency and drug content

The optimized nanoparticles of CSP (CPGE and CPGN) were analyzed for drug entrapment efficiency and drug loading content by HPLC **(Fig. S2)**. The drug entrapment efficiency of CPGE and CPGN were found to be 48.63 ± 4.14 % and 45.13 ± 3.25 %, respectively. Similarly, the percentage of drug loading content for CPGE and CPGN were 5.67 ± 0.52 % and 5.38 ± 0.33 %, respectively (Table 1).

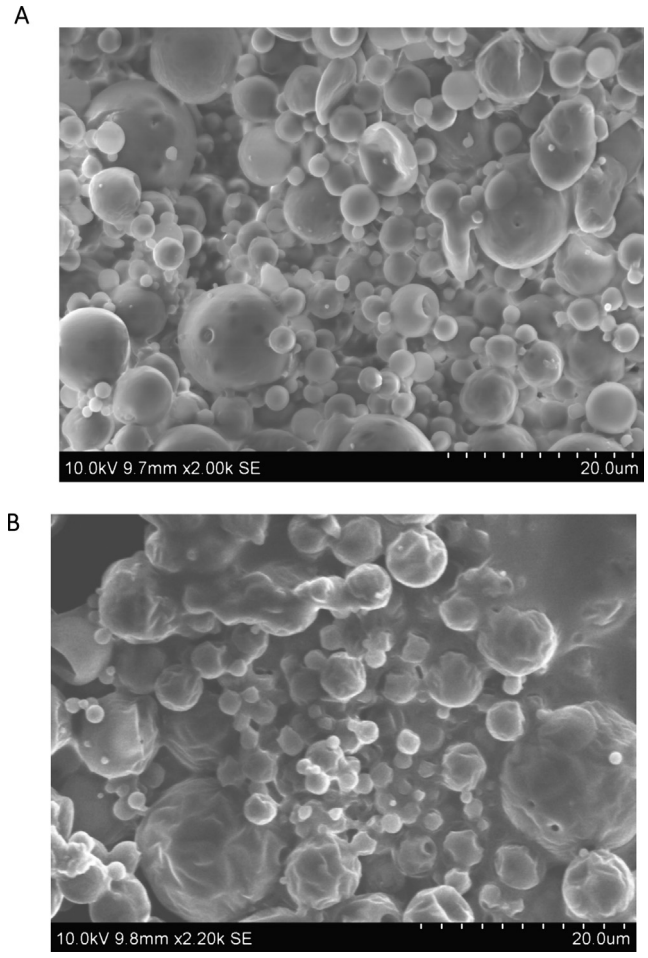

Fig. 2. Cisplatin nanoparticles have smooth surface properties with discrete particle size. The surface morphology of cisplatin n anoparticles (CPGE and CPGN) were examined using SEM. **A** Surface morphology of CPGE nanoparticles**B**. Surface morphology of CPGN nanoparticles. The images are representative of three independent experiments.

3.3. Cisplatin nanoparticles have smooth surface properties with discrete particle size

The surface morphology of the optimized CSP nanoparticles (CPGE and CPGN) were studied using scanning electron microscopy (SEM). Interestingly, the SEM analysis revealed that CPGE and CPGN nanoparticles have spherical and smooth surface properties (Fig. 2). Thus, this data revealed that CSP nanoparticles have discrete particle size and were found to be readily dispersible after lyophilization.

3.4. Cisplatin nanoparticles show initial burst effect followed by the sustained drug release

The drug release characteristics of CSP nanoparticles (CPGE and CPGN) and free CSP were investigated using the dialysis sac method in vitro. The data of in vitro drug release kinetics were expressed as a cumulative percentage of CSP release over time. Interestingly, we found a biphasic pattern characterized by an initial burst effect with a rapid release of the drug during the first 24 h (Fig. 3). In the following period, the release of CSP was in a sustained manner from the nanoparticulate system. Three days of incubation caused 60% of drug release, followed by a slower and continuous release of CSP for 8 days. In contrast, free CSP showed a total release of 90% in the first 2 h, followed by a complete release of the drug in 2 days (Fig. 3). Thus, these data indicated that CSP release from the polymeric nanoparticles were in a sustained release pattern and might be useful as a controlled drug delivery system of anticancer drugs.

3.5. Cisplatin nanoparticles impart cytotoxic effects in human glioblastoma cells

To investigate the cytotoxicity of CSP nanoparticles (CPGE and CPGN), human glioblastoma cells (U-343 and LN-229) were treated with CPGE, CPGN, free CSP (positive control), and blank NPs (vehicle control) for 48 h and 96 h, respectively. Following this, cell viability was gauged by MTT-based assay. Interestingly, in comparison with the free drug (CSP), CSP-NPs imparted cytotoxicity in human glioblastoma cells in a concentration-dependent manner (Fig. 4). At 48 h of treatment, the IC_{50} values of CSP, CPGE,

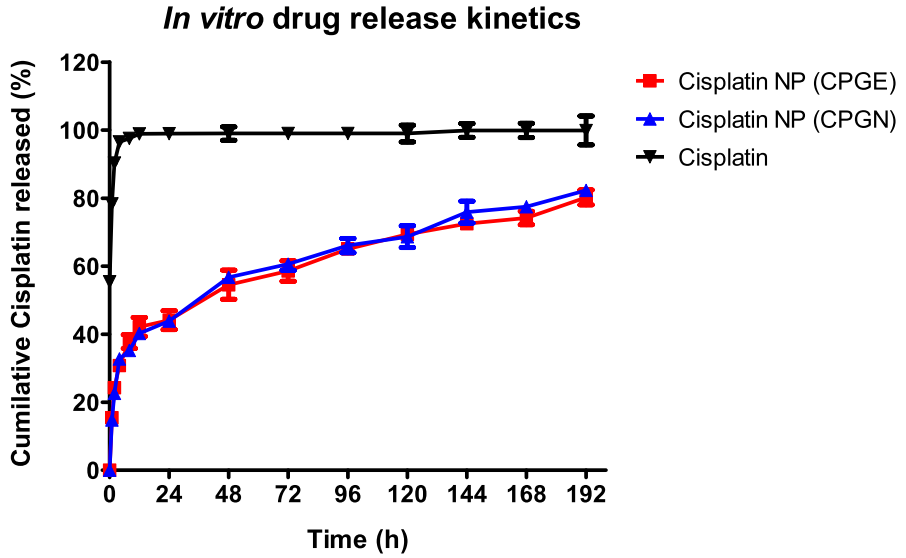

Fig. 3. Cisplatin nanoparticles show an 'initial burst effect' followed by the sustained drug release. Drug release characteristics of cisplatin nanoparticles (CPGE and CPGN) were determined by the dialysis sac method. The drug release study of free cisplatin was performed under the same condition. Results of *in vitro* drug release kinetics were graphically shown as cumulative percentage cisplatin release vs. time. Each point represents the mean ± SEM of three independent experiments performed in triplicates.

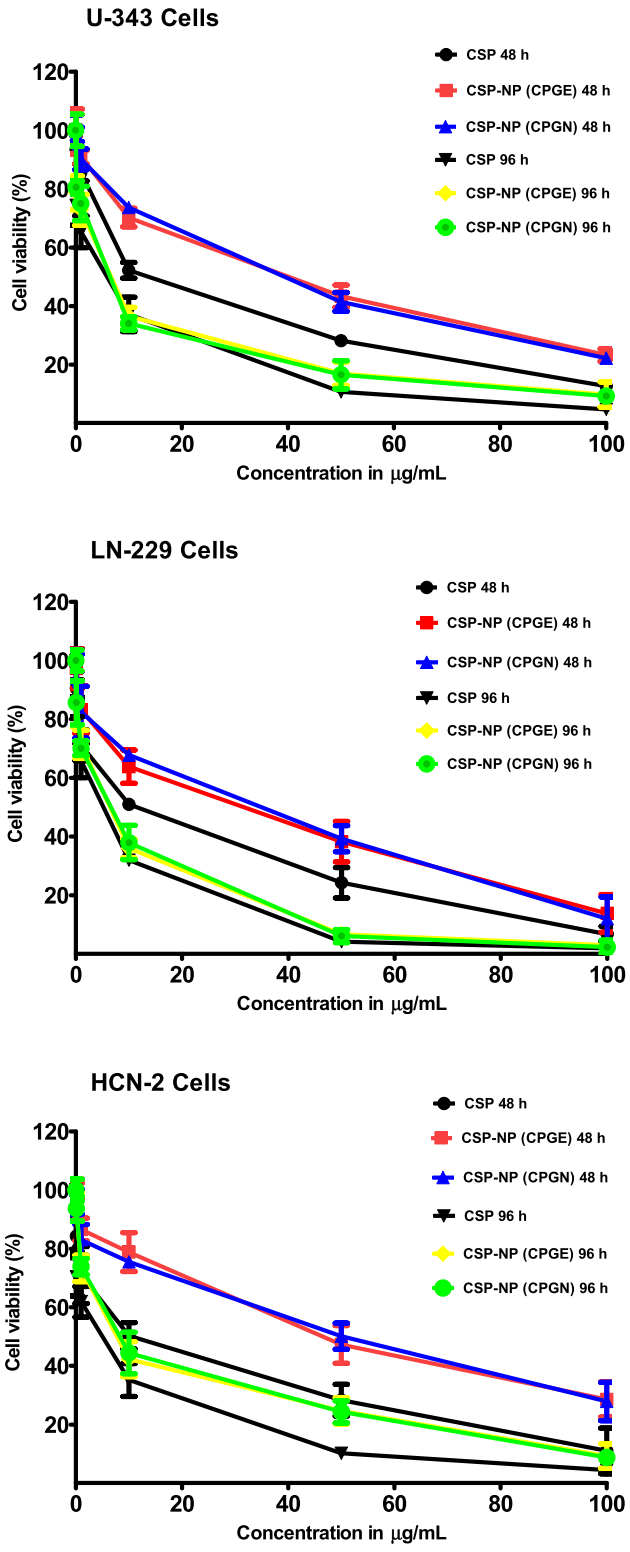

Fig. 4. Cisplatin nanoparticles impart cytotoxic effects in human glioblastoma cells. Human glioblastoma cells (U-343 and LN-229) and human normal brain neuronal cells (HCN-2) were treated with free cisplatin (CSP), cisplatin nanoparticles (CPGE and CPGN), and blank nanoparticles (vehicle control) for 48 h and 96 h, respectively. At the end of the treatment, the percentage of cell viability was determined using MTT assay. IC_{50} (concentration of the drug required to reduce the percentage of cell viability to 50) was obtained from the graph by non-linear regression analysis as curve-fit models using GraphPad Software. Each point represents the mean ± standard error of the mean of three independent experiments performed in triplicates.

and CPGN in U-343 cells were 12.66 ± 0.80 μg/mL, 30.81 ± 2.57 μg/mL, and 30.70 ± 2.92 μg/mL, respectively (Table 2). Similarly, the IC_{50} values of CSP, CPGE, and CPGN in LN-229 cells were 9.18 ± 0.80 μg/mL, 20.76 ± 1.66 μg/mL, and 22.33 ± 1.81 μg/mL, respectively (Table 2). However, at longer incubations of 96 h, we found a significantly enhanced cytotoxic effect for CSP-NPs in cancer cells compared to 48 h of treatment (Fig. 4). The IC_{50} values of CSP, CPGE, and CPGN in U-343 cells at 96 h were 3.24 ± 0.25 μg/mL, 4.79 ± 0.32 μg/mL, and 4.58 ± 0.35 μg/mL, respectively (Table 2). Similarly, the IC_{50} values of CSP, CPGE, and CPGN in LN-229 cells at 96 h were 2.63 ± 0.15 μg/mL, 3.83 ± 0.25 μg/mL, and 3.91 ± 0.30 μg/mL, respectively (Table 2). Thus, this data revealed that in contrast to 48 h of treatment, CSP nanoparticles produced enhanced cytotoxic effects at the chronic treatment of 96 h.

Next, we have investigated the cytotoxic effects of CSP nanoparticles in normal (non-cancerous) cells. Accordingly, human brain cortical neuronal cells (HCN-2) were treated with CSP, CPGE, and CPGN for 48 h and 96 h, respectively. Following this, cell viability was gauged by MTT-based assay. The IC_{50} values of CSP, CPGE, and CPGN in HCN-2 (at 48 h) were 10.08 ± 0.55 μg/mL, 40.80 ± 1.65 μg/mL, and 40.64 ± 1.50 μg/mL, respectively (Table 2). Similarly, the IC_{50} values of CSP, CPGE, and CPGN in HCN-2 (at 96 h) were 2.38 ± 0.10 μg/mL, 7.18 ± 0.45 μg/mL, and 7.75 ± 0.50 μg/mL, respectively (Table 2). The IC_{50} values of CSP-NPs were higher in HCN-2 cells as compared to U-343/LN-229 cells at both 48 and 96 h treatments. Similarly, the IC_{50} values of CSP-NPs were higher as compared to free cisplatin (CSP) in HCN-2 cells (Fig. 4; Table 2). Thus, these data revealed that CSP-NPs are relatively less cytotoxic in normal brain neuronal cells (HCN-2).

3.6. Cisplatin nanoparticles trigger apoptosis in human glioblastoma cells

The induction of apoptosis was measured using Hoechst 33342 assay. Human glioblastoma cells (U-343 and LN-229) were treated with CSP nanoparticles (CPGE and CPGN) for 96 h. CSP and blank NPs were used as controls. Interestingly, the treatment with CSP nanoparticles exhibited the condensed nuclei, fragmented DNA, and chromatin condensation, indicating apoptosis (Fig. 5). Therefore, this data indicated that the cytotoxic activity of CSP nanoparticles was mediated by triggering apoptosis in human glioblastoma cells.

3.7. Effects of cisplatin nanoparticles in cancer cell cycle

To study the cell cycle-specific effects and mechanisms of cytotoxicity of CSP nanoparticles, human glioblastoma cells (U-343 and LN-229) with CSP nanoparticles (CPGE and CPGN) for 96 h. CSP and blank NPs were used as controls. A clear normal cell cycle profile with G_0/G_1 phase, Synthetic (S) phase, G_2/M phase, without any significant apoptotic phase (sub-G_0 content) was seen in blank NPs (Fig. 6). Conversely, CSP significantly augmented the sub-G_0 content (1.53 ± 0.06 to 14.26 ± 0.15 in U-343 cells and 1.23 ± 0.04 to 17.12 ± 0.53 in LN-229 cells), indicating the induction of apoptosis mediated cell death (Fig. 6; Table 3). Similarly, CPGE and CPGN significantly enhanced the sub-G_0 content (1.53 ± 0.06 to 20.77 ± 0.90 and 1.53 ± 0.06 to 22.38 ± 1.40 in U-343 cells, respectively; 1.23 ± 0.04 to 24.99 ± 1.22 and 1.23 ± 0.04 to 26.98 ± 3.52 in LN-229 cells, respectively) (Fig. 6; Table 3). The sub-G_0 content was relatively high in CPGE, and CPGN treated samples as compared to CSP alone. However, we could not detect any significant G_0/G_1 or G_2/M arrest. Therefore, these data corroborated that CSP nanoparticles augmented apoptosis mediated cell death in cancer cells.

Table 2
Cytotoxicity of cisplatin nanoparticles in human glioblastoma cells. Human glioblastoma cells (U-343 and LN-229) and human normal brain neuronal cells (HCN-2) were treated with free cisplatin (CSP) and cisplatin nanoparticles (CPGE and CPGN) for 48 h and 96 h, respectively. Blank nanoparticles were used as vehicle control. At the end of the treatment, the percentage of cell viability was determined by MTT assay. IC_{50} (concentration of the drug required to reduce the percentage of cell viability to 50) was obtained from the graph (Figure 4) by non-linear regression analysis as best curve-fit models using GraphPad Prism Software. Numerical data represent the mean ± standard error of the mean of three independent experiments. Two-Way ANOVA, followed by 'Bonferroni post-tests,' was used to determine the statistically significant IC_{50} values for cisplatin NPs treatment at 48 h versus 96 h. 1) U-343 and LN-229 cells (***P < 0.001). 2) HCN-2 cells as compared to U-343/LN-229 cells at 48 h (***P < 0.001). 3) HCN-2 cells as compared to U-343/LN-229 cells 96 h (**P < 0.01).

IC_{50} (μg/mL)	U-343 (48 h)	LN-229 (48 h)	U-343 (96 h)	LN-229 (96 h)	HCN-2 (48 h)	HCN-2 (96 h)
Cisplatin (CSP)	12.66 ± 0.80	9.18 ± 0.80	3.24 ± 0.25	2.63 ± 0.15	10.08 ± 0.55	2.38 ± 0.10
Cisplatin-NP (CPGE)	30.81 ± 2.57	20.76 ± 1.66	4.79 ± 0.32***	3.83± 0.25***	40.80 ± 1.65***	7.18± 0.45**
Cisplatin-NP (CPGN)	30.70 ± 2.92	22.33 ± 1.81	4.58 ± 0.35***	3.91 ± 0.30***	40.64 ± 1.50***	7.75± 0.50**

3.8. Cisplatin nanoparticles enhance the drug uptake in human glioblastoma cells

Since CSP nanoparticles increased apoptosis in cancer cells, particularly at chronic incubations, we undertook experiments to assess the intracellular uptake of CSP nanoparticles in cancer cells. Accordingly, CSP cellular content was measured indirectly using DOX fluorescence. Briefly, human glioblastoma cells (U-343 and LN-229) were treated with CSP nanoparticles (CPGE and CPGN), CSP (positive control), and blank NPs (vehicle control) in the presence of a sub-lethal concentration of DOX for 96 h. Following treatment, cellular uptake of CSP was monitored visually using a fluorescent microscope. In control experiments (vehicle control), we observed extremely low fluorescence **(**Fig. 7 **A)**. However, the treatment of cells with CSP showed cellular uptake of cisplatin in the presence of DOX **(**Fig. 7 **B)**. Interestingly, the treatment of cells with cisplatin nanoparticles (CPGE and CPGN) revealed significantly enhanced intracellular drug accumulations (fluorescence appeared to be in both cytoplasm and nuclei) **(**Fig. 7 **C and D)**. Thus, these data revealed that CSP nanoparticles increased the cellular uptake and accumulation in cancer cells as compared to free CSP.

3.9. Cisplatin nanoparticles augment drug accumulation in human glioblastoma cells

Next, we investigated the accumulation of CSP nanoparticles in human glioblastoma cells using flow cytometry-based experiments. Human glioblastoma cells (U-343 and LN-229) were incubated with free cisplatin and CSP nanoparticles (CPGE and CPGN) in the DNR accumulation phase. At the end of the treatment, the mean fluorescent intensity (MFI) of DNR as an indicator of quantitative CSP accumulations in the cancer cells were measured using flow cytometry. The intracellular accumulation of free cisplatin (measured as MFI of DNR) was 142.4 ± 10.47 and 145.2 ± 13.13 in U-343 and LN-229 cells, respectively (Fig. 8). However, the MFI for CPGE and CPGN in U-343 cells were 261.6 ± 8.54 and 258.9 ± 9.95, respectively. Similarly, the MFI for CPGE and CPGN in LN-229 cells were 251.6 ± 12.48 and 231 ± 11.58, respectively (Fig. 8). Therefore, these data revealed that as compared to free cisplatin, the treatment of cancer cells with CSP nanoparticles significantly augmented the intracellular accumulation of CSP in human GBM cells. These results also suggest that consistent with enhanced uptake of CSP nanoparticles in cancer cells, CSP nanoparticles also caused significant accumulation of anticancer drug (DNR) in human GBM cells.

3.10. Cisplatin nanoparticles inhibit multidrug resistance transporter (ABCB1 or p-glycoprotein)

Next, we investigated the potential of CSP nanoparticles to inhibit the drug efflux transporters, particularly MDR transporters such as ABCB1 and ABCG2. The ability of CSP nanoparticles to block the ABCB1 mediated drug transport was assessed by the Rho-123 assay. Accordingly, human glioblastoma cells (U-343 and LN-229) were treated with CSP alone, CSP nanoparticles (CPGE and CPGN), and verapamil (positive control for ABCB1 inhibition). At the end of the treatments, drug efflux characteristics were measured by flow cytometry. The mean fluorescent intensity (MFI) of Rho-123 in the CSP treated samples were 408.7 ± 30.09 and 345.0 ± 22.95 in U-343 and LN-229 cells, respectively (Fig. 9). However, verapamil caused significantly increased the MFI of Rho-123 (408.7 ± 30.09 to 921. 0 ± 28.47 and 345.0 ± 22.95 to 841.3 ± 37.69) in U-343 and LN-229 cells, respectively (Fig. 9). A significantly increased MFI of Rho-123 indicates the inhibition of ABCB1 mediated drug transport in the cells. In comparison with free cisplatin (CSP), treatment with CSP nanoparticles caused significantly increased MFI of Rho-123 in both cell types (In U-343 cells, 408.7 ± 30.09 to 665.2 ± 31.33 for CPGE; 408.7 ± 30.09 to 673.1 ± 46.02 for CPGN) (In LN-229 cells, 345.0 ± 22.95 to 572.0 ± 27.82 for CPGE; 345.0 ± 22.95 to 537.6 ± 39.52 for CPGN). In comparison with verapamil, the relative inhibition of ABCB1 for CPGE and CPGN (in U-343 cells) were 72.22% and 73.08%, respectively. Similarly, the relative inhibition of ABCB1 for CPGE and CPGN in LN-229 cells was 67.99% and 63.90%, respectively. Hence, these data corroborated that CSP nanoparticles significantly blocked the ABCB1 activity in human glioblastoma cells.

3.11. Cisplatin nanoparticles inhibit multidrug resistance transporter (ABCG2 or BCRP)

The mitoxantrone (MX) efflux assay was used to assess the ABCG2 inhibitory effects of CSP nanoparticles. Human glioblastoma cells (U-343 and LN-229) were treated with CSP alone, CSP nanoparticles (CPGE and CPGN), and fumitremorgin C (FTC). The functional activities of ABCG2 were evaluated by flow cytometry. A significantly enhanced mean fluorescent intensity (MFI) of MX in the presence of the FTC/test compound is an indication of inhibition of ABCG2 mediated drug transport in the cancer cells. The MFI in the CSP treated sample was 70.84 ± 6.78 (in U-343 cells). However, the treatment with FTC caused a significant increase in the MFI to 219.2 ± 11.20 **(**Fig. 10**)**. As compared to free cisplatin, CSP nanoparticles produced significantly enhanced MFI in the cancer cells (171.1 ± 8.34 and 142.8 ± 11.11 for CPGE and CPGN, respectively). **(**Fig. 10**)**. Similarly, in LN-229 cells, As compared to free cisplatin, CSP nanoparticles caused significantly increased MFI of MX (109.5 ± 7.03 to 387.4 ± 22.09 for FTC; 109.5 ± 7.03 to 216.4 ± 15.72 for CPGE; 109.5 ± 7.03 to 219.2 ± 11.20 for CPGN) **(**Fig. 10**)**. In comparison with FTC, the relative inhibition of ABCG2 (in U-343 cells) for CPGE and CPGN was 78.05% and 65.14%. Similarly, the relative restraint of ABCG2 in LN-229 cells was 55.85% and 56.58%. Therefore, these data corroborated that CSP nanoparticles significantly inhibited the MDR transporters (ABCG2) and caused intracellular accumulation of MX in human glioblastoma cells.

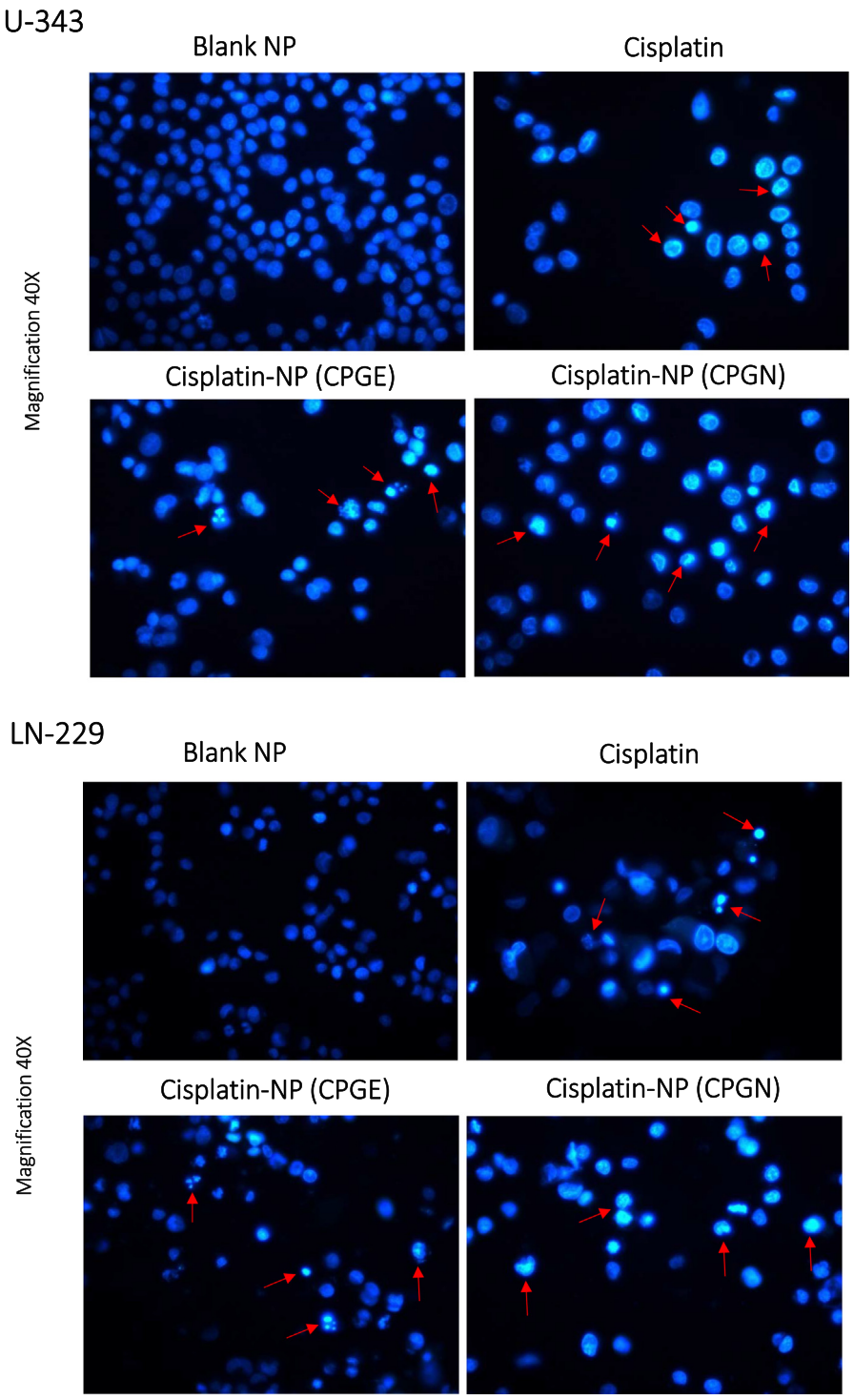

Fig. 5. Cisplatin nanoparticles trigger apoptosis in human glioblastoma cells. Human glioblastoma cells (U-343 and LN-229) were treated with free cisplatin (CSP), cisplatin nanoparticles (CPGE and CPGN), and blank nanoparticles (vehicle control) for 96 h. At the end of the treatment, cells were stained with Hoechst 33342 for detection of apoptosis. Morphological features of apoptosis were gauged using fluorescent microscopy. The images are representative of three independent experiments at a magnification of 40X.

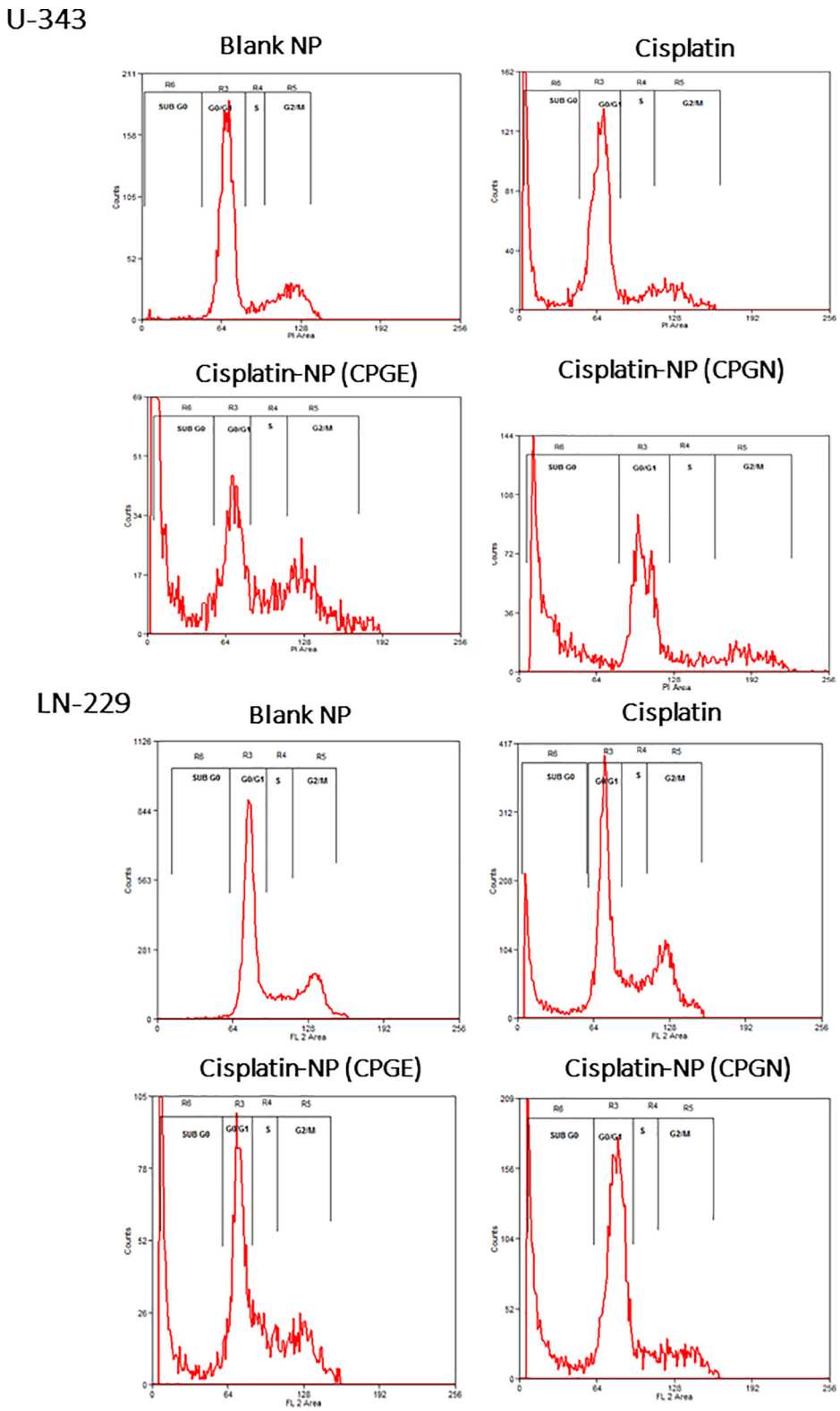

Fig. 6. Effects of cisplatin nanoparticles in the cancer cell cycle. Human glioblastoma cells (U-343 and LN-229) were treated with free cisplatin (CSP), cisplatin nanoparticles (CPGE and CPGN), and blank nanoparticles (vehicle control) for 96 h. At the end of the treatment, cells were harvested, stained with propidium iodide (PI), and DNA content was analyzed using flow cytometry. The percentage of DNA content in G_0/G_1, S, G_2M, and sub-G_0 was determined. The data is representative of three independent experiments.

Table 3
Cell cycle-specific pharmacological effects of cisplatin nanoparticles in human glioblastoma cells. Human glioblastoma cells (U-343 and LN-229) were treated with free cisplatin (CSP), cisplatin nanoparticles (CPGE and CPGN), and blank nanoparticles (vehicle control) for 96 h. Cell cycle analysis was performed based on propidium iodide (PI) staining using flow cytometry at the end of the treatment. The percentage of DNA content in G_0/G_1, S, G_2M, and sub-G_0 phase in U-343 and LN-229 cells were determined (Figure 6). Numerical data are means standard error of the mean of three independent experiments The p-value (***$p < 0.001$) indicates statistical significance for treated groups compared to the blank nanoparticles, determined by Two-Way ANOVA followed by 'Bonferroni post-tests' using GraphPad Software.

	U-343				LN-229			
	Sub G_0 phase	G_o/G_1 phase	S phase	G_2/M phase	Sub G_0 phase	G_o/G_1 phase	S phase	G_2/M phase
Blank NP	1.53 ± 0.06	68.90 ± 5.10	4.75 ± 0.90	23.73 ± 2.50	1.23 ± 0.04	60.79 ± 6.20	12.55 ± 2.10	25.52 ± 1.30
Cisplatin (CSP)	14.26 ± 0.15***	25.97 ± 3.50	3.37 ± 0.48	5.80 ± 5.90	17.12 ± 0.53***	45.12 ± 3.00	12.03 ± 0.40	26.91 ± 4.80
Cisplatin-NP (CPGE)	20.77 ± 0.90***	11.38 ± 4.20	4.73 ± 0.70	8.29 ± 3.11	24.99 ± 1.22***	34.87 ± 3.20	13.26 ± 1.30	19.18 ± 1.85
Cisplatin-NP (CPGN)	22.38 ± 1.40***	39.11 ± 5.80	4.46 ± 1.20	12.35 ± 2.52	26.98 ± 3.52***	47.84 ± 5.70	6.65 ± 0.90	12.00 ± 2.25

4. Discussion

CSP is an anticancer drug commonly used in the treatment of various solid tumors. Yet, the clinical exploitation of CSP is constrained by its toxicity in healthy cells, low bioavailability, and the development of drug resistance. GBM remains the most challenging type of tumor with an inadequate response to CSP chemotherapy (Hanif et al., 2017). The objective of this study was to study the prospect of specific delivery of CSP to human GBM cells that relied on the nanoparticulate system using PLGA as a carrier. In contrast to healthy cells, tumor cells have leaky microvasculature, and hence it is anticipated that nanoparticles of CSP could accumulate to a greater extent in GBM cells (Avgoustakis et al., 2002). PLGA is an active and clinically proven biodegradable polymeric carrier for the enhanced delivery of anticancer drugs as they are efficient, biocompatible, impart sustained release effects, and enhances the accumulation of drugs in tumors by minimizing side effects (Shavi et al., 2015; Musmade et al., 2014). Hence, the incorporation of CSP into PLGA systems as a nanoparticulate drug delivery system will increase the effective delivery of CSP in GBM cells with fewer effects in non-cancerous cells. The unique size of CSP nanoparticles, high surface-volume ratio, enhanced permeability retention (EPR) effects, tumor extravasation, self-assembly, and specificity makes them attractive in passive drug targeting (Patel et al., 2019). Further, CSP PLGA nanoparticles may enhance the circulation time and deliver the CSP to GBM cells by reducing cellular uptake to the endocytic route and thereby eliminating normal tissue toxicity. In this study, we have prepared the CSP PLGA nanoparticles (CSP PLGA NP) by double emulsion (w/o/w) method and nanoprecipitation techniques. The nanoparticles were characterized for particle size (PS), zeta potential (ZP), polydispersity index (PDI), drug entrapment efficiency, and drug loading content. The optimized batches of CSP nanoparticles (CPGE and CPGN) were studied for drug release kinetics and cytotoxicity in human GBM cells using in vitro models. The anticancer mechanisms of CSP nanoparticles in human GBM cells were investigated by apoptosis assay, cell cycle analysis, drug uptake assay, drug accumulation analysis, and drug efflux assay.

We have used two protocols in the formulation and development of CSP nanoparticles. The entrapment of drugs in a drug delivery system is mainly determined by the solubility of the drug and polymer. The drug (CSP) is soluble aqueous solution, whereas the polymer (PLGA) is soluble in organic solvents. Therefore, modified double emulsion (w/o/w) solvent evaporation and nanoprecipitation (solvent diffusion) methods were used for the formulation of CSP nanoparticles. These methods were used to analyze the influence of formulation variables for desired PS, surface morphology, ZP, PDI, drug entrapment efficiency, and drug loading content. CSP to PLGA ratio, organic to aqueous phase ratio, sonication speed/magnitudes/time, type of surface-active agents, and concentration of surfactants were optimized to get desirable PS (0–200 nm), PDI (<0.1), ZP (>minus 20), encapsulation efficiency (>40%), drug loading (>5%) and surface characteristics. During the formulation and development phase, we found that the optimized drug to polymer and solvent to non-solvent ratio were 1:10, probe sonication amplitude was 80 with a pulse of 4 sec for 10 min with stirring speed of 1000 rpm, concentration of sodium cholate (surfactant) was 1% w/v, and the concentration of mannitol (lyoprotectant) was 5% w/v. Among the various batches of CSP nanoparticles prepared, CPGE, which is prepared by modified double emulsion procedure, and CPGN, which is developed by the nanoprecipitation technique, was found to have desired PS, ZP, PDI, drug entrapment efficiency, and drug loading content. Interestingly, we found that the modified double emulsion method has resulted in smaller PS and better drug loading content as compared to the double emulsion method used previously. Similarly, the modified double emulsion method has produced significantly lower PS as compared to the nanoprecipitation technique. This may be because the modified double emulsion method makes the CSP NP more hydrophilic, which increases the penetration of water from the peripheral aqueous phase, thus facilitating drug dissolution and leakage from the NP during formulations. However, we could find any significant change in ZP, PDI, drug entrapment efficiency, and drug loading efficiency for CSP NP formulated by the modified double emulsion in comparison with nanoprecipitation.

The quantification of CSP by the suitable analytical method was challenging due to a lack of chromophore or detectable ions. One of the strategies used for the estimation of CSP was derivatization with diethyldithiocarbamate (DDTC) to produce the CSP-DDTC complex and thereby estimating total platinum content (Zahednezhad et al., 2020). However, these methods have numerous limitations in the detection of CSP in nanoparticulate systems and biological fluids. Therefore, we have developed a sensitive and accurate HPLC system for the quantification of CSP in the CSP NP without any derivatization. This assay was validated for specificity, linearity, and limit of detection. CSP was well-resolved at a retention time of 5.60 min at detection of 305 nm. Therefore, in our experiments, we have used this HPLC method for the estimation of CSP in the nanoparticulate system. In vitro drug release kinetics study of CSP NP revealed a biphasic release pattern with the 'initial burst release effects' followed by drug delivery in a sustained fashion over an extensive phase of 192 h. In contrast to free CSP (~80% of drug release at 1 h), ~70% of encapsulated CSP were released only at 120 h. This drug release model from the CSP NP is useful in the active delivery of CSP in a controlled manner (Reardon et al., 2017). The CSP release from the PLGA NP system during the initial phase is determined by CSP solubility and desorption from the PLGA system (Malinovskaya et al., 2017). However, during the later period, drug release is defined by diffusion and degradation (Malinovskaya et al., 2017). The initial burst release effect may be due to the instant release of CSP remained on the surface of NP and was dependent on drug encapsulation efficiency and drug to polymer ratio used in the formulation. CSP NP formulated with polyvinyl alcohol (PVA) has exhibited a high drug release as

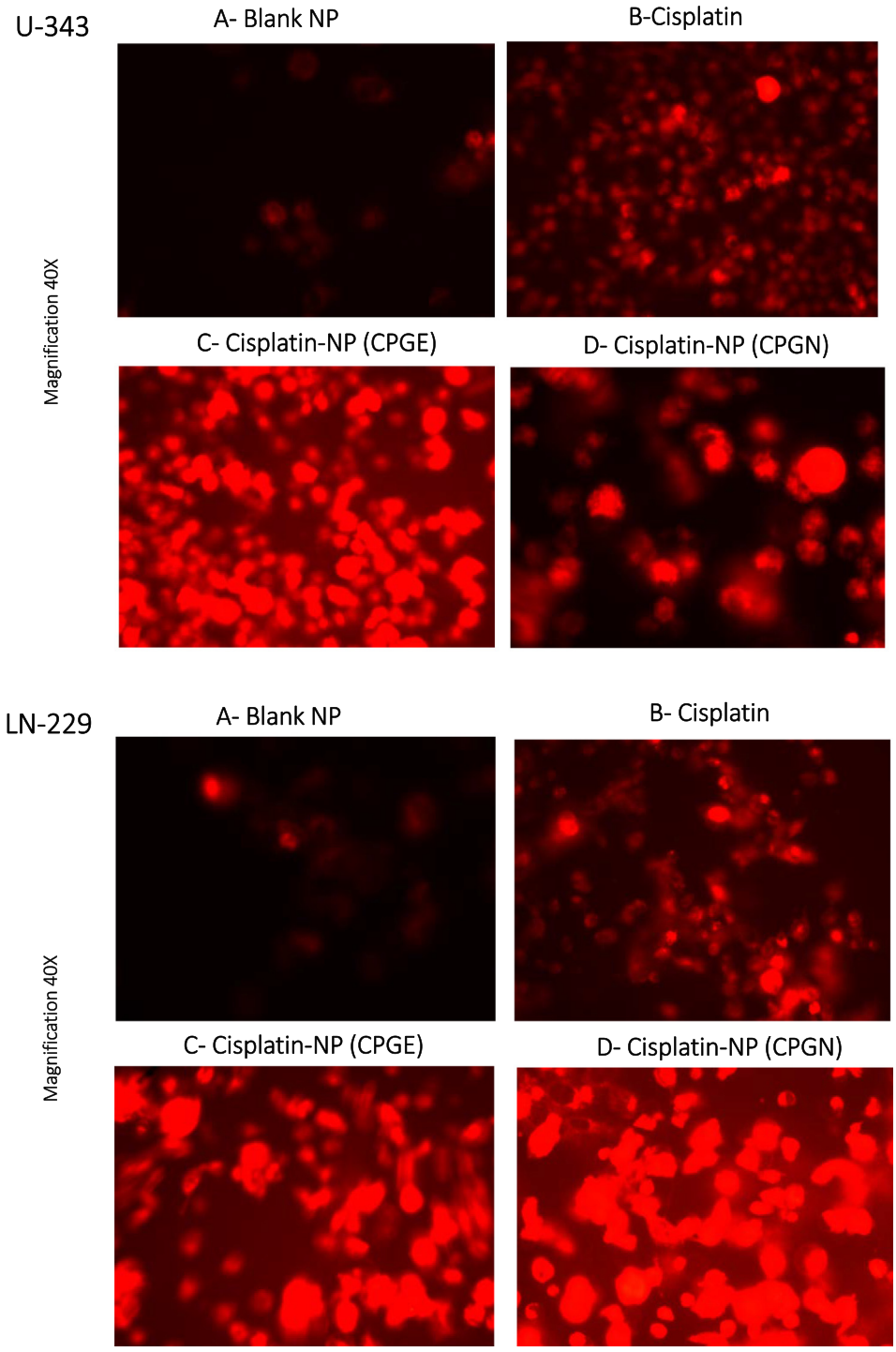

Fig. 7. Cisplatin nanoparticles enhance the drug uptake in human glioblastoma cells. Human glioblastoma cells (U-343 and LN-229) were treated with free cisplatin (CSP), cisplatin nanoparticles (CPGE and CPGN), and blank nanoparticles (vehicle control) in the presence of a of DOX for 96 h. At the end of the treatment, cellular uptake and trafficking of DOX were monitored using a fluorescent microscope. The data is representative of three independent experiments at a magnification of 40X.

compared to sodium cholate. This may be due to the better interface of CSP with polymer matrix and the proper blending of drug and polymer in the oil phase (Shavi et al., 2015). We found that CSP to PLGA ratio at 1: 10, the drug release rate is optimal, as is evident from the SEM analysis that nanoparticles had a smooth surface property. Further, the non-linear form of the graph indicates that CSP nanoparticles go along with 'Higuchi release kinetics' and fit with Ritger-Korsemeyer-Peppas mathematical model (Shavi et al., 2015).

Cytotoxic effects of CSP nanoparticles in human GBM cells (U-343 and LN-229 cells) were evaluated at two different time points (48 h and 96 h) treatment. We found that CSP nanoparticles imparted less cytotoxic effects as compared to free CSP at 48 h at equivalent doses, which follows previous reports (Li et al., 2008). This may be due to the core–shell structure of PLGA nanoparticles and controlled delivery of CSP, ultimately resulting in the slow release of CSP into the culture medium. If cells are treated with CSP nanoparticles for prolonged periods, the CSP concentration

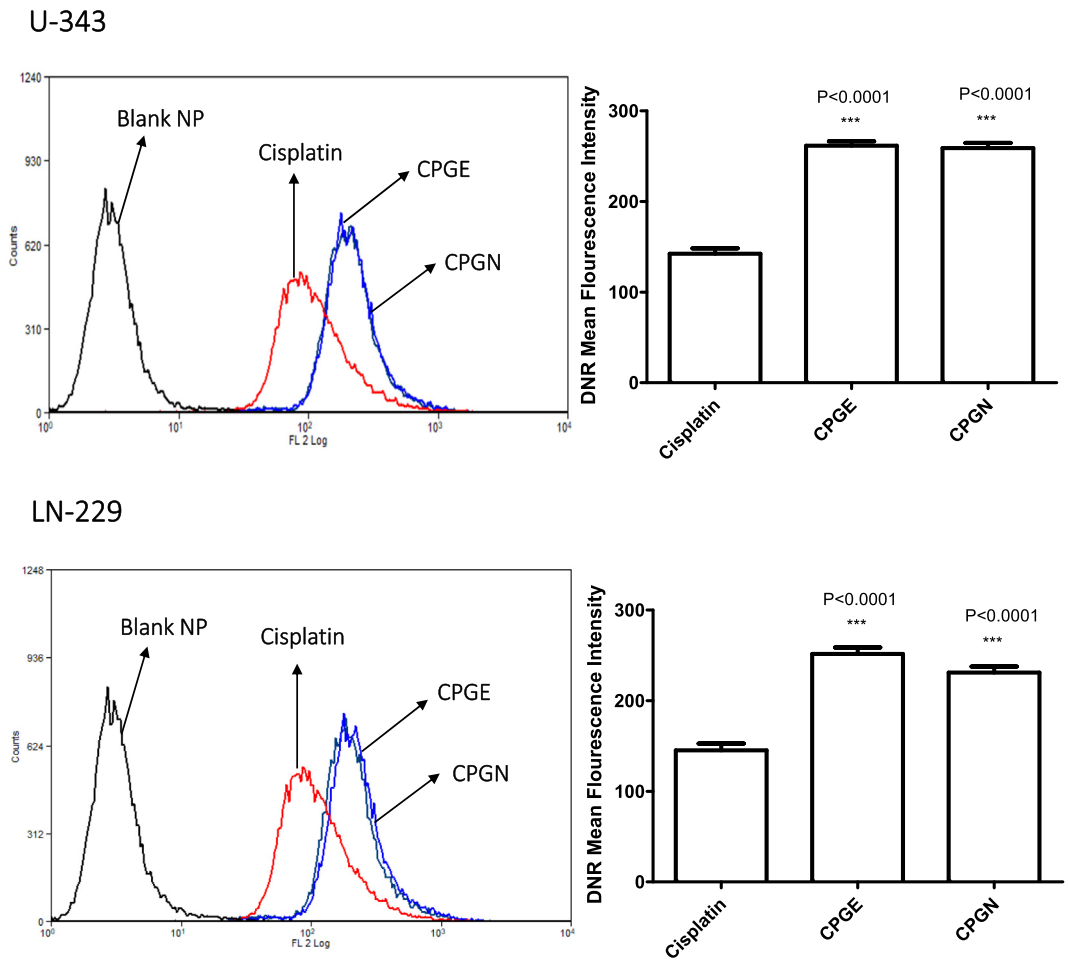

Fig. 8. Cisplatin nanoparticles augment drug accumulation in human glioblastoma cells. Human glioblastoma cells (U343 and LN229) in DMEM with 2% FBS were incubated with free cisplatin (CSP), cisplatin nanoparticles (CPGE and CPGN), and blank nanoparticles (vehicle control) in the presence of DNR for 90 min at 37 °C (Accumulation phase). Cells were washed with HBSS, and the mean fluorescent intensity (MFI) of DNR was measured using flow cytometry. The overlay histograms are representative of three independent experiments. Each point in the bar graph represents the mean ± standard error of the mean of three independent experiments. The p-value (*** p<0.0001) indicates statistical significance for cisplatin nanoparticles compared to the cisplatin, determined by One-Way ANOVA followed by 'Dunnett's Multiple Comparison Test' using GraphPad Prism 5.

may increase owing to the sustained release characteristics (Li et al., 2008). Therefore, we did an extended treatment of GBM cells with CSP-NPs for 96 h. Interestingly, at a treatment period of 96 h, CSP-NPs produced enhanced cytotoxic effects in human GBM cells as compared to 48 h treatment. This may be explained as time-dependent properties for 1. polymer degradation, 2. sustained release of nanoparticles, 3. cell-dependent effects, and 4. intrinsic effect of CSP (Moreno et al., 2010). The drug release kinetics data had indicated that only ~ 65% of CSP was released at 96 h. However, the cytotoxicity assay at long-term treatment (96 h) revealed that CSP nanoparticles imparted similar IC50 as compared to free CSP. Thus, these data suggest that CSP nanoparticles exert relatively more cytotoxicity on cancer cells as compared to free CSP at 96 h, as ~ 35% of the drug remains unreleased from the nanoparticulate system at 96 h. This may be due to the enhanced uptake of nanoparticles by cancer cells and sustained release properties of PLGA based nanoparticles. Interestingly, we found that in contrast to free CSP, CSP nanoparticles failed to impart significant cytotoxicity in healthy brain neuronal cells (non-cancerous cells) as compared to human GBM cells. The decreased IC50 values for cisplatin nanoparticles in normal cells at the 96 h of treatment may be due to the increased amount of cisplatin released from the polymeric system as compared to 48 h, thus exerting the cytotoxicity. However, the cisplatin nanoparticles produced significantly higher IC50 values in normal cells as compared to cancer cells or free cisplatin, indicating that nanoparticles have less cytotoxicity on healthy brain neuronal cells. This may be explained by the effects of the polymeric system (PLGA is non-toxic and biodegradable), and they can penetrate and accumulate in the cancer cells with less cytotoxic effects on normal cells (Moreno et al., 2010; Patel et al., 2019).

Inducers of apoptosis in cancer cells have attracted a good interest in the development of anticancer agents (Maliyakkal et al., 2013). Since the cytotoxicity data indicated a similar cytotoxic profile between free CSP and CSP nanoparticles at 96 h, the apoptosis assay and cell cycle analysis were fixed at 96 h. Hoechst 33342 assay revealed the CSP nanoparticles induced apoptosis, which was comparable with free CSP treatments. Further, cell cycle analysis and quantitative estimation of apoptosis (by measuring sub G_0 DNA content) revealed that treatments with CSP nanoparticles produced a relatively high sub G_0 phase (indicating apoptosis) as compared to free CSP. However, we could detect any significant cell cycle arrest at any phase. The SubG_0 peak was evident with the loss of populations from the G_0/G_1 and G_2/M phase. Therefore, our results corroborated that CSP nanoparticles significantly induced apoptosis in human GBM cells. These enhanced anticancer effects of CSP nanoparticles may be due to the enhanced drug uptake. Therefore, we assessed the intracellular accumulation of CSP

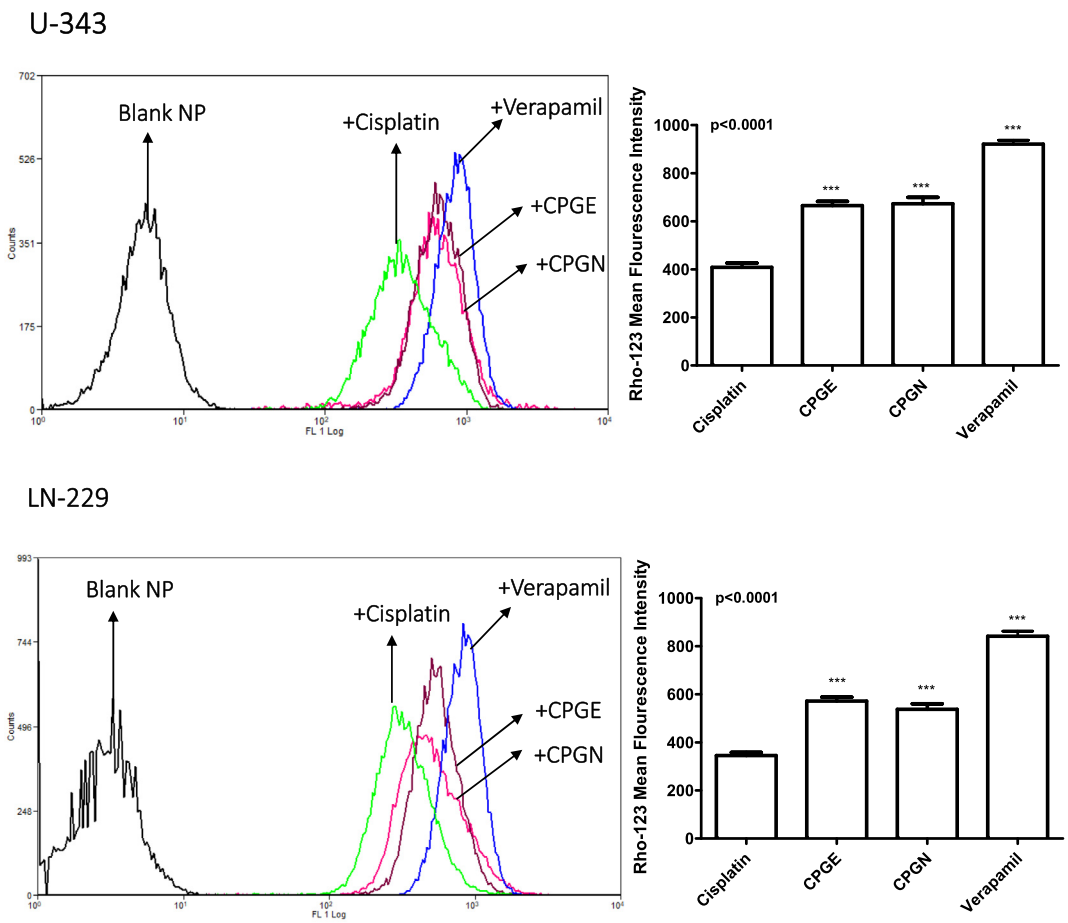

Fig. 9. Cisplatin nanoparticles inhibit multidrug resistance transporter (ABCB1 or p-glycoprotein). Human glioblastoma cells (U343 and LN229) cells in DMEM with 2% FBS were incubated with Rho-123 for 30 min at 37 °C; after which cells were washed and re-incubated with free cisplatin (CSP), cisplatin nanoparticles (CPGE and CPGN), blank nanoparticles (vehicle control), and verapamil (positive control) for 60 min at 37 °C (efflux phase). The mean cellular Rho-123 fluorescence in the efflux phase with cisplatin, cisplatin nanoparticles (CPGE and CPGN), and verapamil were analyzed by flow cytometry. The overlay histograms are representative of three independent experiments. Each point in the bar graph represents the mean ± standard error of the mean of three independent experiments. The p-value (*** p<0.0001) indicates statistical significance for treated groups compared to the free cisplatin, determined by One-Way ANOVA followed by 'Dunnett's Multiple Comparison Test' using GraphPad Prism 5.

nanoparticles in cancer cells based on the fluorescent microscopy-based assay. Our data shows that the treatment of cancer cells with CSP nanoparticles significantly augmented the drug retention in the presence of DOX. Similarly, the flow cytometry based DNR accumulation assay also indicated that CSP nanoparticles caused significant drug accumulations in cancer cells. This enhanced uptake and intracellular accumulations of CSP nanoparticles may be due to the characteristics of nanoparticles, such as nanoparticle size, sustained-release effects, and specific uptake of nanoparticles by cancer cells through the inhibition of drug efflux transporters present in the cancer cell membrane (Sharma et al., 2018).

Drug resistance remains a significant obstacle in CSP based chemotherapy (Ghosh, 2019). CSP resistance is due to the reduced influx and increased efflux of CSP, which ultimately diminishes drug retention in cancer cells (Duan et al., 2016). Among the numerous mechanisms of CSP resistance, the involvement of multidrug resistance proteins (MRPs), a drug efflux transporter, has attracted wide interest. MRPs causes the efflux of CSP outside the cell leading to the diminished intracellular concentration of drugs (Farooq et al., 2019). Recent reports have demonstrated that platin-M (CSP prodrug) nanoparticles loaded into PLGA-PEG, allowed intra-mitochondrial delivery of CSP in neuroblastoma cells to overcome drug resistance, thereby enhanced drug retention in the brain without neurotoxicity (Marrache et al., 2014). However, there is no study reported which investigates the potential of CSP nanoparticles to inhibit the drug efflux transporters. In our experiments, since the CSP nanoparticles caused enhanced uptake and accumulations of anticancer drugs (DOX and DNR) in cancer cells, we have undertaken experiments to assess the potential of these nanoparticles to reverse the functional activity of MDR transporters. Thus, the ability of CSP nanoparticles to inhibit the functional activities of ABCB1 (p-glycoprotein) and ABCG2 (BCRP) were assessed using Rho-123 and MX efflux assays (Beeran et al., 2014). The potential of CSP nanoparticles to reverse these MDR transporter's activities in cancer cells were performed in comparison with standards, such as verapamil (inhibitor of ABCB1) and FTC (inhibitor of ABCG2). Interestingly, our results revealed that CSP nanoparticles caused significant inhibition of ABCB1 and ABCG2 in human GBM cells. Further, it was found that nanoparticles produced 60–75% of relative inhibition of ABCB1 as compared to verapamil. Similarly, as compared to FTC, CSP nanoparticles have shown 55–78% of relative inhibition of ABCG2 in human GBM cells. Therefore, it was found that CSP nanoparticles reverse the MDR in human GBM cells by enhancing drug accumulation, inhibiting drug efflux mechanisms via ABC transporters, such as ABCB1 and ABCG2.

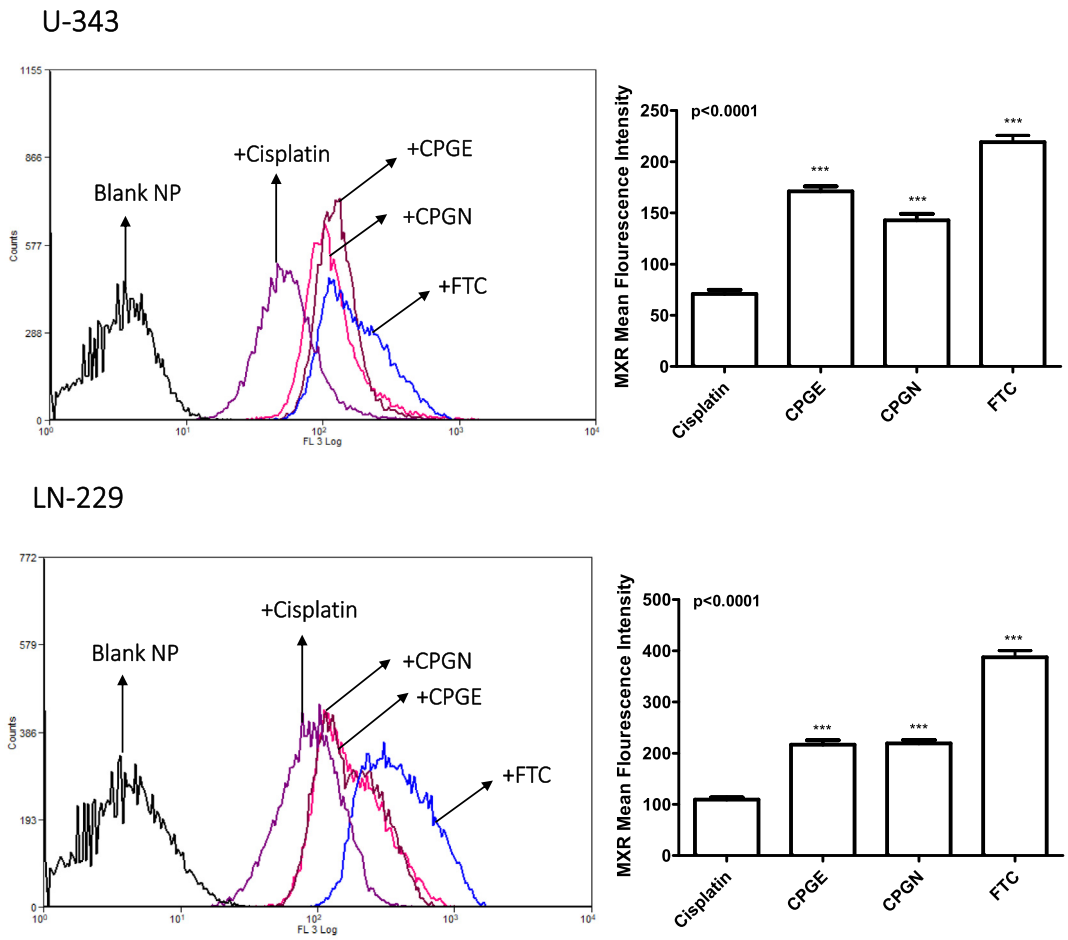

Fig. 10. Cisplatin nanoparticles inhibit multidrug resistance transporter (ABCG2 or BCRP). Human glioblastoma cells (U343 and LN229) cells in DMEM with 2% FBS were incubated with MX for 30 min at 37 °C; after which cells were washed and re-incubated with free cisplatin (CSP), cisplatin nanoparticles (CPGE and CPGN), blank nanoparticles (vehicle control), and fumitremorgin C (positive control) for 60 min at 37 °C (efflux phase). The mean cellular MX fluorescence in the efflux phase with cisplatin, cisplatin nanoparticles (CPGE and CPGN), and fumitremorgin C were analyzed by flow cytometry. The overlay histograms are representative of three independent experiments. Each point in the bar graph represents the mean ± standard error of the mean of three independent experiments. The p-value (*** p<0.0001) indicates statistical significance for treated groups compared to the free cisplatin, determined by One-Way ANOVA followed by 'Dunnett's Multiple Comparison Test' using GraphPad Prism 5.

5. Conclusion

CSP is a conventionally used chemotherapeutic drug routinely used in the treatment of solid tumors. However, the clinical effectiveness of CSP in GBM is reduced, owing to the inability to cross the blood–brain barrier, toxic side effects, drug resistance, and relapse. We have designed and developed the nanoplatform of CSP with the PLGA system to improve the delivery of CSP to GBM, thus reducing adverse effects and toxicities. The present study demonstrates that this nanoplatform of CSP has excellent encapsulation efficiency, desired particle size, and sustained drug release properties. In vitro cytotoxicity assay revealed that CSP nanoparticles impart cytotoxic effects in human GBM without affecting normal brain cortical neuronal cells. Further, studies have corroborated that CSP nanoparticles augmented apoptosis and enhanced cellular uptake and intracellular drug accumulations, which enables the effective delivery of the CSP into the human GBM cells, thus offering its therapeutic outcome. More interestingly, CSP nanoparticles inhibited the MDR transporters such as ABCB1 and ABCG2, thus enabling the blockade of the drug efflux mechanism. Chemoresistance remains a limitation for the successful treatment of GBM, and the inhibition of the MDR mechanisms by CSP nanoparticles could be a favorable alternative for the effective treatment of GBM. Thus, this study found a promising method for the effective delivery of CSP in GBM cells, resulting in enhanced therapeutic effects and minimizing adverse effects. However, this nanoplatform warrants further research to depict the relationship between the physicochemical characteristics of CSP-NPs and the mechanisms of the actions of MDR. Further in vivo studies using mouse xenograft models may lead to the biodistribution characteristics of CSP-NPs, its ability to cross the BBB, drug uptake/retention mechanisms, in vivo pharmacokinetics, and drug release kinetics with tumor interactions. Thus, this study enlightens the viability and benefits of selective targeting of CSP in clinical applications.

Data availability

All data generated or analyzed during this study are included in this published article (and its supplementary information files).

Funding

The authors extend their appreciation to the Deanship of Scientific Research (DSR) at King Khalid University (KKU), Abha, Kingdom of Saudi Arabia, for funding this work through the General Research Project under the grant number G.R.P-333-39.

Declaration of Competing Interest

The authors declare that they have no known competing financial interests or personal relationships that could have appeared to influence the work reported in this paper.

Acknowledgments

The authors extend their appreciation to the Deanship of Scientific Research (DSR) at King Khalid University (KKU), Abha, Kingdom of Saudi Arabia, for funding this work through the General Research Project under the grant number G.R.P-333-39.

We would like to acknowledge Dr. Devaveena Dey (Assistant Professor, USU Walter Reed Surgery, Uniformed Services University of the Health Sciences, Bethesda, MD, USA) for technical editing, reviewing, and revising the manuscript. The authors also acknowledge Dr. Gopal Shavi (Principal Professional, LEO Pharma A/S, Crumlin Dublin, Ireland) and Dr. Praful Deshpande (Lead Scientist, Teva Pharmaceuticals, Waterford Metropolitan Area, Ireland) for their help with formulation and development.

Appendix A. Supplementary data

Supplementary data to this article can be found online at https://doi.org/10.1016/j.jsps.2021.07.001.

References

Alam, N., Koul, M., Mintoo, M.J., Khare, V., Gupta, R., Rawat, N., Sharma, P.R., Singh, S. K., Mondhe, D.M., Gupta, P.N., 2017. Development and characterization of hyaluronic acid modified PLGA based nanoparticles for improved efficacy of cisplatin in solid tumor. Biomed. Pharmacother. 95, 856–864.

Anthony, C., Mladkova-Suchy, N., Adamson, D.C., 2019. 17The evolving role of antiangiogenic therapies in glioblastoma multiforme: Current clinical significance and future potential. Expert Opin. Investig. Drugs 28 (9), 787–797.

Averineni, Ranjith K, Shavi, Gopal V, Gurram, Aravind K, Deshpande, Praful B, Arumugam, Karthik, Maliyakkal, Naseer, Meka, Sreenivasa R, Nayanabhirama, Udupa, 2012. PLGA 50:50 nanoparticles of paclitaxel: Development, in vitro anti-tumor activity in BT-549 cells and in vivo evaluation. Bull. Mater. Sci. 35 (3), 319–326.

Avgoustakis, K., Beletsi, A., Panagi, Z., Klepetsanis, P., Karydas, A.G., Ithakissios, D.S., 2002. PLGA-mPEG nanoparticles of cisplatin: in vitro nanoparticle degradation, in vitro drug release and in vivo drug residence in blood properties. J. Control. release 79, 123–135.

Bar-Zeev, M., Livney, Y.D., Assaraf, Y.G., 2017. Targeted nanomedicine for cancer therapeutics: towards precision medicine overcoming drug resistance. Drug Resist. Updat. 31, 15–30.

Appadath Beeran, Asmy, Maliyakkal, Naseer, Rao, Chamallamudi Mallikarjuna, Nayanabhirama, Udupa, 2015. The enriched fraction of Elephantopus scaber Triggers apoptosis and inhibits multi-drug resistance transporters in human epithelial cancer cells. Pharmacogn. Mag. 11 (42), 257–268.

Appadath Beeran, A., Maliyakkal, N., Rao, C.M., Udupa, N., 2014. The enriched fraction of Vernonia cinerea L. induces apoptosis and inhibits multi-drug resistance transporters in human epithelial cancer cells. J. Ethnopharmacol. 158, 33–42.

Cheng, L., Jin, C., Lv, W., Ding, Q., Han, X.u., 2011. Developing a highly stable PLGA-mPEG nanoparticle loaded with cisplatin for chemotherapy of ovarian cancer. PLoS One 6 (9), e25433.

Cheng, Q., Shi, H., Huang, H., Cao, Z., Wang, J., Liu, Y., 2015. Oral delivery of a platinum anticancer drug using lipid assisted polymeric nanoparticles. Chem. Commun. 51 (99), 17536–17539.

Dhar, S., Gu, F.X., Langer, R., Farokhzad, O.C., Lippard, S.J., 2008. Targeted delivery of cisplatin to prostate cancer cells by aptamer functionalized Pt (IV) prodrug-PLGA-PEG nanoparticles. Proc. Natl. Acad. Sci. 105 (45), 17356–17361.

Domínguez-Ríos, R., Sánchez-Ramírez, D.R., Ruiz-Saray, K., Oceguera-Basurto, P.E., Almada, M., Juárez, J., Zepeda-Moreno, A., del Toro-Arreola, A., Topete, A., Daneri-Navarro, A., 2019. Cisplatin-loaded PLGA nanoparticles for HER2 targeted ovarian cancer therapy. Colloids Surfaces B Biointerfaces 178, 199–207.

Duan, X., He, C., Kron, S.J., Lin, W., 2016. Nanoparticle formulations of cisplatin for cancer therapy. Wiley Interdiscip. Rev. Nanomedicine Nanobiotechnology 8 (5), 776–791.

El-khateeb, M., Appleton, T.G., Charles, B.G., Gahan, L.R., 1999. Development of HPLC conditions for valid determination of hydrolysis products of cisplatin. J. Pharm. Sci. 88 (3), 319–326.

Farooq, M.A., Aquib, M.d., Farooq, A., Haleem Khan, D., Joelle Maviah, M.B., Sied Filli, M., Kesse, S., Boakye-Yiadom, K.O., Mavlyanova, R., Parveen, A., Wang, B.o., 2019. Recent progress in nanotechnology-based novel drug delivery systems in designing of cisplatin for cancer therapy: an overview. Artif. Cells, Nanomedicine, Biotechnol. 47 (1), 1674–1692.

Ghosh, S., 2019. Cisplatin: The first metal based anticancer drug. Bioorg. Chem. 88, 102925. https://doi.org/10.1016/j.bioorg.2019.102925.

Gryparis, E.C., Hatziapostolou, M., Papadimitriou, E., Avgoustakis, K., 2007. Anticancer activity of cisplatin-loaded PLGA-mPEG nanoparticles on LNCaP prostate cancer cells. Eur. J. Pharm. Biopharm. 67 (1), 1–8.

Hanif, F., Muzaffar, K., Perveen, K., Malhi, S.M., Simjee, S.U., 2017. Glioblastoma multiforme: a review of its epidemiology and pathogenesis through clinical presentation and treatment. Asian Pacific J. cancer Prev. APJCP 18, 3.

Hartshorn, C.M., Bradbury, M.S., Lanza, G.M., Nel, A.E., Rao, J., Wang, A.Z., Wiesner, U. B., Yang, L., Grodzinski, P., 2018. Nanotechnology strategies to advance outcomes in clinical cancer care. ACS Nano 12 (1), 24–43.

Heffron, T.P., 2016. Small molecule kinase inhibitors for the treatment of brain cancer. J. Med. Chem. 59 (22), 10030–10066.

Li, X., Li, R., Qian, X., Ding, Y., Tu, Y., Guo, R., Hu, Y., Jiang, X., Guo, W., Liu, B., 2008. Superior antitumor efficiency of cisplatin-loaded nanoparticles by intratumoral delivery with decreased tumor metabolism rate. Eur. J. Pharm. Biopharm. 70 (3), 726–734.

Liao, W., Fan, S., Zheng, Y., Liao, S., Xiong, Y., Li, Y.i., Liu, J., 2019. Recent advances on glioblastoma multiforme and nano-drug carriers: A review. Curr. Med. Chem. 26 (31), 5862–5874.

Malinovskaya, Y., Melnikov, P., Baklaushev, V., Gabashvili, A., Osipova, N., Mantrov, S., Ermolenko, Y., Maksimenko, O., Gorshkova, M., Balabanyan, V., Kreuter, J., Gelperina, S., 2017. Delivery of doxorubicin-loaded PLGA nanoparticles into U87 human glioblastoma cells. Int. J. Pharm. 524 (1-2), 77–90.

Maliyakkal, N., Appadath Beeran, A., Balaji, S.A., Udupa, N., Ranganath Pai, S., Rangarajan, A., 2015. Effects of withania somnifera and tinospora cordifolia extracts on the side population phenotype of human epithelial cancer cells: Toward targeting multidrug resistance in cancer. Integr. Cancer Ther. 14 (2), 156–171.

Maliyakkal, N., Udupa, N., Pai, K.S.R., Rangarajan, A., 2013. Cytotoxic and apoptotic activities of extracts of withania somnifera and tinospora cordifolia in human breast cancer cells. Int. J. Appl. Res. Nat. Prod. 6, 1–10.

Marrache, S., Pathak, R.K., Dhar, S., 2014. Detouring of cisplatin to access mitochondrial genome for overcoming resistance. Proc. Natl. Acad. Sci. 111 (29), 10444–10449.

Masood, F., 2016. Polymeric nanoparticles for targeted drug delivery system for cancer therapy. Mater. Sci. Eng. C 60, 569–578.

Mattheolabakis, G., Taoufik, E., Haralambous, S., Roberts, M.L., Avgoustakis, K., 2009. In vivo investigation of tolerance and antitumor activity of cisplatin-loaded PLGA-mPEG nanoparticles. Eur. J. Pharm. Biopharm. 71 (2), 190–195.

Miladi, K., Sfar, S., Fessi, H., Elaissari, A., 2016. In: Polymer Nanoparticles for Nanomedicines. Springer International Publishing, Cham, pp. 17–53. https://doi.org/10.1007/978-3-319-41421-8_2.

Miller, M.A., Zheng, Y.-R., Gadde, S., Pfirschke, C., Zope, H., Engblom, C., Kohler, R.H., Iwamoto, Y., Yang, K.S., Askevold, B., Kolishetti, N., Pittet, M., Lippard, S.J., Farokhzad, O.C., Weissleder, R., 2015. Tumour-associated macrophages act as a slow-release reservoir of nano-therapeutic Pt (IV) pro-drug. Nat. Commun. 6 (1). https://doi.org/10.1038/ncomms9692.

Moreno, D., De Ilarduya, C.T., Bandrés, E., Buñuales, M., Azcona, M., Garc'ia-Foncillas, J., Garrido, M.J., 2008. Characterization of cisplatin cytotoxicity delivered from PLGA-systems. Eur. J. Pharm. Biopharm. 68, 503–512.

Moreno, Daniel, Zalba, Sara, Navarro, Iñigo, Tros de Ilarduya, Conchita, Garrido, María J., 2010. Pharmacodynamics of cisplatin-loaded PLGA nanoparticles administered to tumor-bearing mice. Eur. J. Pharm. Biopharm. 74 (2), 265–274.

Musmade, Kranti P., Deshpande, Praful B., Musmade, Prashant B., Maliyakkal, M. Naseer, Kumar, A. Ranjith, Reddy, M. Sreenivasa, Udupa, N., 2014. Methotrexate-loaded biodegradable nanoparticles: Preparation, characterization and evaluation of its cytotoxic potential against U-343 MGa human neuronal glioblastoma cells. Bull. Mater. Sci. 37 (4), 945–951.

Patel, Param, Hanini, Anas, Shah, Achal, Patel, Dhruv, Patel, Shyam, Bhatt, Priyanka, Pathak, Yashwant V, 2019. In: Surface Modification of Nanoparticles for Targeted Drug Delivery. Springer International Publishing, Cham, pp. 19–31. https://doi.org/10.1007/978-3-030-06115-9_2.

Reardon, P.J.T., Parhizkar, M., Harker, A.H., Browning, R.J., Vassileva, V., Stride, E., Pedley, R.B., Edirisinghe, M., Knowles, J.C., 2017. Electrohydrodynamic fabrication of core shell PLGA nanoparticles with controlled release of cisplatin for enhanced cancer treatment. Int. J. Nanomedicine 12, 3913.

Risnayanti, C., Jang, Y.-S., Lee, J., Ahn, H.J., 2018. PLGA nanoparticles co-delivering MDR1 and BCL2 siRNA for overcoming resistance of paclitaxel and cisplatin in recurrent or advanced ovarian cancer. Sci. Rep. 8, 1–12.

Robey, Robert W., Pluchino, Kristen M., Hall, Matthew D., Fojo, Antonio T., Bates, Susan E., Gottesman, Michael M., 2018. Revisiting the role of ABC transporters in multidrug-resistant cancer. Nat. Rev. Cancer 18 (7), 452–464.

Sharma, Ankush, Goyal, Amit K., Rath, Goutam, 2018. Recent advances in metal nanoparticles in cancer therapy. J. Drug Target. 26 (8), 617–632.

Shavi, Gopal Venkatesh, Nayak, Usha Yogendra, Maliyakkal, Naseer, Deshpande, Praful Balavant, Raghavendra, Ramesh, Kumar, Averineni Ranjith, Reddya, Meka Sreenivasa, Udupa, Nayanabhirama, Shrawan, B., 2015. Nanomedicine of anastrozole for breast cancer: Physicochemical evaluation, in vitro cytotoxicity on BT-549 and MCF-7 cell lines and preclinical study on rat model. Life Sci. 141, 143–155.

Tian, Jing, Min, Yuanzeng, Rodgers, Zachary, Au, Kin Man, Hagan, C. Tilden, Zhang, Maofan, Roche, Kyle, Yang, Feifei, Wagner, Kyle, Wang, Andrew Z., 2017. Co-delivery of paclitaxel and cisplatin with biocompatible PLGA-PEG nanoparticles enhances chemoradiotherapy in non-small cell lung cancer models. J. Mater. Chem. B 5 (30), 6049–6057.

Wang, Yunfei, Liu, Peifeng, Qiu, Lihua, Sun, Ying, Zhu, Mingjie, Gu, Liying, Di, Wen, Duan, Yourong, 2013. Toxicity and therapy of cisplatin-loaded EGF modified mPEG-PLGA-PLL nanoparticles for SKOV3 cancer in mice. Biomaterials 34 (16), 4068–4077.

Xu, X., Xie, K., Zhang, X.-Q., Pridgen, E.M., Park, G.Y., Cui, D.S., Shi, J., Wu, J., Kantoff, P.W., Lippard, S.J., Langer, R., Walker, G.C., Farokhzad, O.C., 2013. Enhancing tumor cell response to chemotherapy through nanoparticle-mediated codelivery of siRNA and cisplatin prodrug. Proc. Natl. Acad. Sci. 110 (46), 18638–18643.

Yu, H., Tang, Z., Li, M., Song, W., Zhang, D., Zhang, Y., Yang, Y., Sun, H., Deng, M., Chen, X., 2016. Cisplatin loaded poly (L-glutamic acid)-g-methoxy poly (ethylene glycol) complex nanoparticles for potential cancer therapy: preparation, in vitro and in vivo evaluation. J. Biomed. Nanotechnol. 12, 69–78.

Yu, Minzhi, Yuan, Wenmin, Li, Dan, Schwendeman, Anna, Schwendeman, Steven P., 2019. Predicting drug release kinetics from nanocarriers inside dialysis bags. J. Control. Release 315, 23–30.

Zahednezhad, Fahimeh, Zakeri-Milani, Parvin, Shahbazi Mojarrad, Javid, Valizadeh, Hadi, 2020. The latest advances of cisplatin liposomal formulations: essentials for preparation and analysis. Expert Opin. Drug Deliv. 17 (4), 523–541.